ANA CAROLINA CUNHA ARANTES

OBTENÇÃO DE HÍBRIDOS NANOESTRUTURADOS PARA APLICAÇÕES AMBIENTAIS

LAVRAS - MG

2017

Ficha catalográfica elaborada pelo Sistema de Geração de Ficha Catalográfica da Biblioteca Universitária da UFLA, com dados informados pelo(a) próprio(a) autor(a).

Arantes, Ana Carolina Cunha.
Obtenção de híbridos nanoestruturados para aplicações ambientais / Ana Carolina Cunha Arantes. - 2017.
63 p. : il.

Orientador(a): Maria Lucia Bianchi.
Coorientador(a): Gustavo Henrique Denzin Tonoli.
Tese (doutorado) - Universidade Federal de Lavras, 2017.
Bibliografia.

1. Biopolímeros. 2. Catálise. 3. Eletrônica. I. Bianchi, Maria Lucia . II. Tonoli, Gustavo Henrique Denzin. III. Título.

ANA CAROLINA CUNHA ARANTES

OBTENÇÃO DE HÍBRIDOS NANOESTRUTURADOS PARA APLICAÇÕES AMBIENTAIS

Tese apresentada à Universidade Federal de Lavras, como parte das exigências do Programa de Pós-Graduação em Agroquímica, área de concentração em Agroquímica, para a obtenção do título de Doutora.

Orientadora
Dra. Maria Lucia Bianchi

Co- orientador
Dr. Gustavo Henrique Denzin Tonoli

LAVRAS - MG

2017

ANA CAROLINA CUNHA ARANTES

OBTENÇÃO DE HÍBRIDOS NANOESTRUTURADOS PARA APLICAÇÕES AMBIENTAIS

Tese apresentada à Universidade Federal de Lavras, como parte das exigências do Programa de Pós-Graduação em Agroquímica, área de concentração em Agroquímica, para a obtenção do título de Doutora.

APROVADA em 17 de fevereiro de 2017.

Dr. Diego Alvarenga Botrel	UFLA
Dra. Eliane Cristina de Resende	IFMG
Dr. Joaquim Paulo da Silva	UFLA
Dr. Lourival Marin Mendes	UFLA

Dra. Maria Lucia Bianchi
Orientadora

Dr. Gustavo Henrique Denzin Tonoli
Co- orientador

LAVRAS - MG

2017

“A melhor coisa que você pode fazer
para cultivar a verdadeira sabedoria
é praticar a consciência
de que o mundo é um sonho.”
-Paramahansa Yogananda-

AGRADECIMENTOS

Agradeço à Ana Carolina, minha companheira, minha amiga, minha confidente, minha parceira. Dividir e viver minha vida com você me ensina e me completa das mais diversas maneiras possíveis. Agradeço aos meus pais, Ronaldo e Virgínia, e minhas irmãs, Paula e Mariane, que sempre estão do meu lado em todas as conquistas da vida, fazendo-as possíveis e sendo meu porto seguro, independente da distância. Eu amo vocês. Agradeço a Deus, onipresente!

Agradeço a Malu, pela caminhada de tantos anos. Ao Gustavo, por me dar um rumo e ser sempre solícito!

Agradeço aos membros da banca por aceitarem o convite.

Agradeço aos meus companheiros de jornada, colegas de laboratório e aos colegas de trabalho. Aos meus amigos de Lavras, de Formiga, e os espalhados por aí. Aos meus familiares que sempre participam das minhas conquistas, cada um com sua contribuição.

Cris, Luiz e Ligiane por toda ajuda! Delilah Wood, amazing person that I had the pleasure of working together. Guerreiro e Lidy pelo CAPQ, Roberta pelas análises de DRX, Luiz pelas análises de BET, Joaquim pelas análises elétricas, Marali pelas análises mecânicas.

À Universidade Federal de Lavras, aos Departamentos de Química, Ciências Florestais, Ciências dos Alimentos e Física pela infraestrutura.

RESUMO

Os materiais híbridos são utilizados em inúmeras aplicações devido à grande versatilidade de composição e síntese. Os híbridos nanoestruturados apresentam pelo menos um de seus componentes em escala nanométrica, o que facilita a dispersão e interação entre os componentes. Os híbridos nanoestruturados podem ser aplicados visando a redução de impactos ambientais causados pela atividade humana, seja na diminuição da geração de resíduos ou no tratamento de resíduos gerados. Para isso os híbridos devem apresentar componentes renováveis, biodegradáveis e de fácil obtenção, que é o caso dos biopolímeros, como a celulose e a quitosana, e os óxidos de ferro, como a magnetita. Nesse contexto essa tese teve como objetivo o desenvolvimento de materiais híbridos para aplicações ambientais. Na primeira parte foi realizada uma revisão bibliográfica sobre materiais híbridos, componentes e aplicações. A segunda parte foi dividida em dois artigos. O primeiro artigo apresenta o desenvolvimento de um catalisador hibrido, em forma de pó, composto de nanofibrilas de celulose e magnetita que foi utilizado em reações do tipo Fenton para degradação do corante modelo azul de metileno visando o tratamento de efluentes de indústrias têxteis. O catalisador apresentou atividade em 10 ciclos consecutivos com degradação total de uma solução de azul de metileno (50 ppm) em 180 minutos. No segundo artigo foi desenvolvido um híbrido, em forma de filme fino, composto de nanofibrilas de celulose, quitosana, magnetita e glicerol, que foi testado para utilização na produção de capacitores visando diminuir a geração de resíduos eletrônicos tóxicos e não renováveis. Os filmes apresentaram constantes dielétricas elevadas em uma frequência de 100 Hz podendo ser utilizados como dielétricos em capacitores.

Palavras-chave: Híbridos; Celulose; Quitosana; Magnetita; Catálise; Eletrônica.

ABSTRACT

Hybrid materials are used in various applications due to the versatility of their compositions and syntheses. The nano scale of nanostructured hybrids facilitates dispersion and interactions of all components in the resulting hybrid material. Nanostructured hybrids may be applied to reduce negative environmental impacts, either by reducing waste during their production or in the treatment of waste streams in production of other materials. The least negative environmental impact dictates that the hybrid material components be renewable, biodegradable and easily obtained. Such materials include biopolymers (cellulose and chitosan) and iron oxides (magnetite). The work for this thesis focused on developing hybrid materials for environmental applications. The first part is a bibliographic review on hybrid materials and their components and applications. The second part was divided into two papers. The first paper presented the development of a hybrid catalyst, composed of cellulose nanofibrils and magnetite to be used in Fenton-like reactions to degrade methylene blue, with the goal of treating textile effluents. The resulting hybrid catalyst retained activity in 10 consecutive cycles resulting in the total degradation of methylene blue solution (50 ppm) in 180 min. The second paper included the development of a thin film hybrid composed of cellulose nanofibrils, chitosan, magnetite and glycerol. The film was developed and tested for use in the production of capacitors in order to reduce the generation of toxic and nonrenewable e-waste. The resulting films had high dielectric constant at a 100 Hz frequency being able to be used as a dielectric in capacitors.

Keywords: Hybrids; Cellulose; Chitosan; Magnetite; Catalysis; Electronics.

SUMÁRIO

INTRODUÇÃO

O estudo de novos materiais engloba as mais diversas áreas do conhecimento e unem pesquisadores com diferentes saberes na busca por alto desempenho e propriedades cada vez mais específicas visando diversas aplicações, como exemplo, desenvolver materiais que auxiliem na diminuição de impactos ambientais causados pela atividade humana. Um impacto ambiental que ocorre na maioria das linhas de produção é a geração de uma grande quantidade de resíduos que necessitam de tratamento e correta disposição.

A produção de têxteis, por exemplo, movimenta diversos setores e gera uma enorme quantidade de efluentes contendo alta carga de contaminantes. O tratamento desses efluentes pode ser feito por meio de reações de degradação utilizando o processo Fenton que é catalisado pelo íon ferro. Outra atividade que gera muitos resíduos é a produção eletroeletrônica e sua participação na indústria tem crescido muito, pois é cada vez maior a necessidade de desenvolver produtos que armazenem grande quantidade de energia e dados, de uma maneira cada vez mais rápida para acompanhar o desenvolvimento tecnológico.

Nesse contexto, os materiais híbridos podem substituir materiais tradicionais visando a solução de problemas ambientais, seja na diminuição da produção de resíduos ou mesmo no tratamento dos resíduos gerados. Para tal é necessário a utilização de precursores renováveis, biodegradáveis e de baixo custo. Um exemplo desses precursores são os biopolímeros, como a celulose e a quitosana, que são abundantes e versáteis, possibilitando o desenvolvimento de diversos tipos de materiais, seja para servirem de matriz ou como suporte para outro componente (por exemplo a magnetita) na produção dos híbridos. Os híbridos podem apresentar diversos formatos, como os aerogéis, xerogéis, pós, filmes finos, membranas, dentre outros.

O presente trabalho se divide em duas partes. Na primeira parte apresenta-se uma revisão bibliográfica sobre os materiais híbridos em geral, alguns componentes para produção de híbridos (celulose, magnetita e quitosana) e suas aplicações ambientais na área de catálise para tratamento de efluentes e na área de eletrônica para armazenamento de carga. Na segunda parte são apresentados dois trabalhos práticos, na forma de artigos científicos, resultantes do estudo da obtenção de híbridos nanoestruturados para aplicações ambientais. No primeiro artigo foi desenvolvido um catalisador híbrido de nanofibrilas de celulose e magnetita que foi utilizado na degradação do corante azul de metileno em reações catalíticas do tipo Fenton. No segundo artigo foram produzidos filmes finos contento celulose, quitosana, magnetita e glicerol para utilização como dielétricos na produção de capacitores.

PRIMEIRA PARTE

1 REFERENCIAL TEÓRICO

1.1 Materiais híbridos

Materiais que possuem pelo menos dois componentes ou duas fases com propriedades físicas e/ou químicas distintas entre si resultam em um material híbrido. Um híbrido pode apresentar propriedades resultantes da soma das contribuições individuais dos componentes ou pode apresentar propriedades distintas resultante do sinergismo entre os componentes (JOSÉ; PRADO, 2005; SALAS et al., 2014; SMALL; JOHNSTON, 2009). Os híbridos podem ser aplicados desde simples materiais até em produtos de alta tecnologia e são utilizados em diversas áreas como medicina, catálise, eletricidade e aeronáutica e de acordo com o objetivo podem possuir propriedades elétricas, magnéticas, mecânicas, dentre outras (CAVALIERI et al., 2014; CHANG; ZHANG, 2011; MALUCELLI et al., 2014; SMALL; JOHNSTON, 2009; TAN et al., 2016).

Os componentes de um híbrido podem ter diferentes funções por exemplo, um componente utilizado como matriz, conferindo estrutura ao material, e outro componente utilizado como fase ativa, conferindo propriedades físicas e/ou químicas específicas ao material (JOHN; THOMAS, 2008; JOSÉ; PRADO, 2005). Existe uma infinidade de precursores que podem ser utilizados na produção dos híbridos (polímeros, cerâmicas, sílica, óxidos, metais) e que permitem desenvolver projetos em diversas áreas (ALHASSEN et al., 2014). Os híbridos nanoestruturados apresentam pelo menos um dos componentes em escala nanométrica (SALAS et al., 2014). A dispersão do componente nanométrico é maior devido a mobilidade das estruturas e interação com espaços vazios da matriz (KO; CHOI, 2013).

A produção dos híbridos pode ser feita por diversos processos (Figura 1) e eles podem apresentar diversos formatos, como exemplo, os xerogéis, produzidos a partir da secagem lenta de uma suspensão dos precursores e os filmes finos que podem ser produzidos por *casting* (MALUCELLI et al., 2014). Alguns componentes são muito utilizados na produção de híbridos como os polímeros naturais, por exemplo, a celulose e a quitosana, e os óxidos de ferro, como a magnetita (TAN et al., 2016).

Figura 1 - Rotas sintéticas de materiais híbridos.

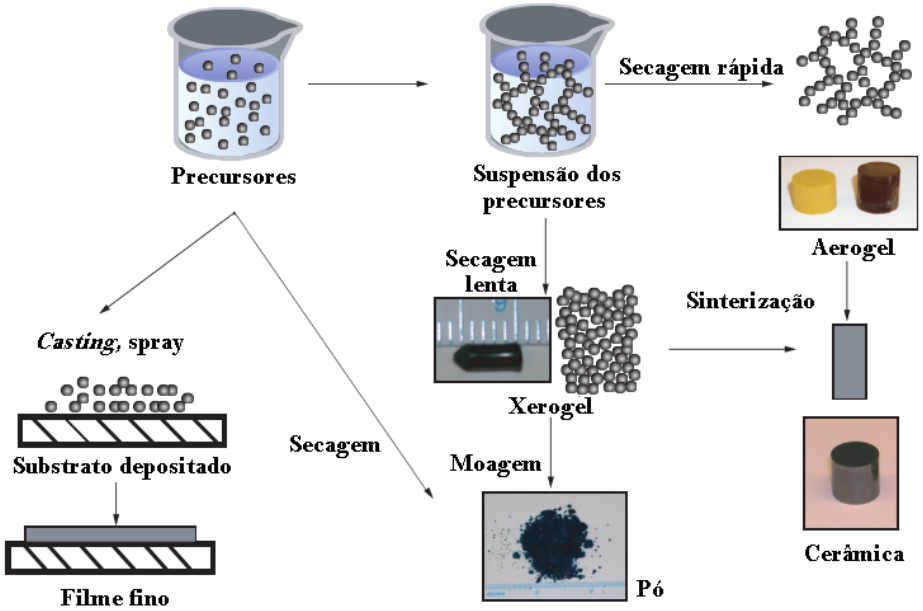

Fonte: Adaptado de Rath (2005).

1.2 Celulose

Os materiais lignocelulósicos, classificados como bio-nanocompósitos (BRINCHI et al., 2013), estão presentes em todas as formas de biomassa vegetal e sua composição básica compreende a celulose, as hemiceluloses e a lignina (BURTON; GIDLEY; FINCHER, 2010; TRACHE et al., 2016). A celulose é considerada o polímero natural mais abundante pois é o componente principal da biomassa vegetal, representando em média 50% da composição da parede celular, sendo que esse teor varia de acordo com a espécie (BRINCHI et al., 2013; EK; GELLERSTEDT; HENRIKSSON, 2009). Além da biomassa vegetal, pode-se obter celulose a partir de resíduos agrícolas, como o bagaço de cana-de-açúcar, palha de milho e fibras diversas (BRINCHI et al., 2013; UMMARTYOTIN; MANUSPIYA, 2015a). Comercialmente, a celulose é utilizada há séculos como matéria prima na produção de papel e tecidos e a produção mundial é estimada em 10^{10} toneladas por ano (ABDUL KHALIL et al., 2014; UMMARTYOTIN; MANUSPIYA, 2015a).

A celulose é uma macromolécula constituída de unidades de β-D-glucopiranose unidas por ligações glicosídicas β-1,4 em um arranjo linear e cristalino (ABDUL KHALIL et al., 2014; BARNETT; JERONIMIDIS, 2003). O monômero da celulose é o dímero da glucose conhecido como celobiose. A Figura 2 representa a celobiose como parte de uma cadeia de celulose em

que n representa o grau de polimerização que é aproximadamente 10.000 unidades para a celulose nativa (WANG; LU; ZHANG, 2016; ZUGENMAIER, 2008).

Figura 2 – Monômero celobiose presente na celulose.

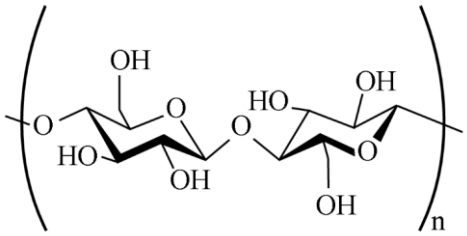

As cadeias de celulose têm uma grande tendência em formar ligações de hidrogênio devido aos grupos hidroxilas presentes nos carbonos secundários e no grupo metilol dos carbonos primários (FENGEL; WEGENER, 1984; WANG; LU; ZHANG, 2016). O grande número de ligações de hidrogênio intra e intermoleculares (Figura 3) faz com que a celulose seja insolúvel em solventes orgânicos, água, ácidos e bases à temperatura ambiente conduzindo a uma limitação de reatividade e processamento (TRACHE et al., 2016; WANG; LU; ZHANG, 2016).

Figura 3 - Representação das ligações de hidrogênio intra e intermoleculares da celulose.

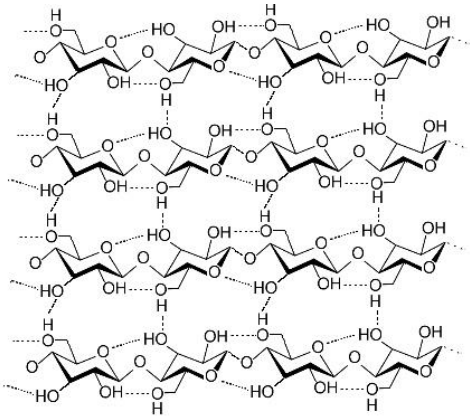

A celulose possui uma função estrutural e é encontrada na parede celular das células vegetais em um conjunto de microfibrilas que se juntam em fibras maiores associadas em uma matriz junto das hemiceluloses e lignina (ABDUL KHALIL et al., 2014). As paredes celulares são organizadas em camadas constituídas por uma lamela média espessa contendo microfibrilas enroladas em forma de hélice, uma parede primária fina com microfibrilas desordenadas e uma

parede secundária constituída de três subcamadas (ABDUL KHALIL; BHAT; IREANA YUSRA, 2012; JOHN; THOMAS, 2008).

Para a obtenção das fibras de celulose a partir dos materiais lignocelulósicos, a biomassa vegetal passa por um tratamento cuja função é deixar as fibras mais acessíveis por meio da remoção da lignina e das hemiceluloses (ABDUL KHALIL et al., 2014; UMMARTYOTIN; MANUSPIYA, 2015a). Esse tratamento pode ocorrer por diversos processos: físicos (picadores, moagem), físico-químicos (explosão a vapor, hidrotermólise), químicos (agentes oxidantes, ácidos diluídos, álcalis, solventes orgânicos) ou biológicos (enzimas, fungos) (BRINCHI et al., 2013; CAPOLUPO; FARACO, 2016; SARKAR et al., 2011; SINGH et al., 2014). Na Figura 4 apresenta-se esquematicamente a maior acessibilidade às fibras de celulose após o tratamento da matéria-prima (KUMAR et al., 2009).

Figura 4 - Efeito do pré tratamento na biomassa.

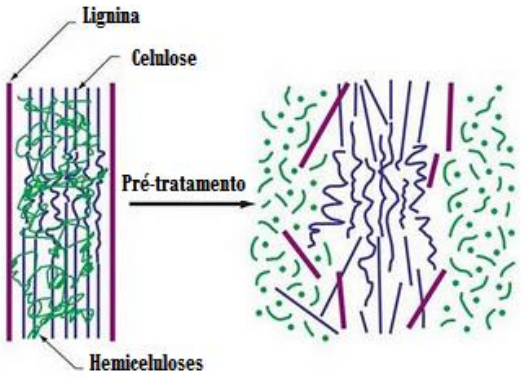

Fonte: Adaptado de Kumar (2009).

1.2.1 Nanofibrilas de celulose

Nanofibrila de celulose pode ser definida como sendo a menor unidade estrutural das fibras vegetais e consiste em feixes de cadeias de celulose que alternam em regiões cristalinas e regiões amorfas (ABDUL KHALIL; BHAT; IREANA YUSRA, 2012; LAVOINE et al., 2012; NECHYPORCHUK; BELGACEM; BRAS, 2016). Outros termos relativo as nanofibrilas de celulose são reportados na literatura, como exemplo os *whiskers*, nanocristais, cristalitos, nanofibras de celulose e nanocelulose sendo que, apesar de serem materiais distintos, possuem em comum pelo menos uma dimensão na escala nanométrica, ou seja, menor que 100nm, variando de acordo com a origem da fibra de celulose utilizada e o método de preparo (ABDUL

KHALIL; BHAT; IREANA YUSRA, 2012; BOUFI et al., 2016). As nanofibrilas de celulose são produzidas a partir das fibras de celulose que já passaram por um tratamento para retirada das hemiceluloses e lignina (TRACHE et al., 2016). Uma grande vantagem de utilizar as nanofibrilas de celulose no desenvolvimento de novos materiais é que elas formam uma suspensão aquosa devido à dimensão nanométrica, facilitando o preparo de híbridos e aumentando a dispersão dos componentes, o que não é possível com as fibras de celulose *in natura*, devido à insolubilidade.

As nanofibrilas de celulose podem ser obtidas de diversas fontes e por diversos processos (ABDUL KHALIL et al., 2014; BOUFI et al., 2016; BRINCHI et al., 2013; LEE et al., 2014; TRACHE et al., 2016). Um dos processos é a hidrólise utilizando ácidos fortes que remove as regiões amorfas das fibras de celulose mantendo as regiões cristalinas o que gera materiais com uma alta razão de aspecto (comprimento/ diâmetro da fibra) (ABDUL KHALIL et al., 2014; LAVOINE et al., 2012; TRACHE et al., 2016). As dimensões das nanofibrilas vão depender da porcentagem de regiões amorfas o que varia para cada biomassa (EICHHORN et al., 2009). Uma desvantagem da hidrólise ácida é a geração de resíduos ácidos e a exigência de uma etapa de purificação do material. Outra forma de obtenção das nanofibrilas é por meio físico. As fibras de celulose, já separadas das hemiceluloses e lignina, passam por uma espécie de moinho, também chamado de *grinder*, onde ocorre uma desfibrilação mecânica decorrente do atrito das partes do moinho (BOUFI et al., 2016; UMMARTYOTIN; MANUSPIYA, 2015a). O resultado é uma suspensão com aspecto de gel formado por fibras com dimensões nanométricas e que não necessita de uma etapa de purificação das fibras (NECHYPORCHUK; BELGACEM; BRAS, 2016; TONOLI et al., 2016).

As nanofibrilas de celulose apresentam características como, leveza, rigidez, boas propriedades mecânicas e óticas, não tóxicas e biodegradáveis, que as tornam um bom precursor para diversos materiais (TRACHE et al., 2016). Alguns materiais que podemos citar são os aerogéis, os xerogéis, e os nanofilmes de celulose.

Os aerogéis de celulose (Figura 5) são obtidos a partir da secagem rápida de uma suspensão de nanofibrilas de celulose, onde ocorre a troca do solvente por ar (KISTLER, 1931), resultando em um material com baixa densidade e alta área superficial (CHIN; BINTI ROMAINOR; PANG, 2014). Estudos mostram diversas aplicações para os aerogéis de celulose (HAN et al., 2016; MULYADI; ZHANG; DENG, 2016; PANZELLA et al., 2016; WAN et al., 2015; YANG et al., 2016) como suporte de nanopartículas (WAN; LI, 2015), atividade

fotocatalítica, aplicação em sensores (ZHOU et al., 2014) e supercapacitores (ZHANG et al., 2014).

Quando a secagem da suspensão de nanofibrilas de celulose for rápida são produzidos os aerogéis. Se a secagem é lenta, o material colapsa e forma um outro tipo de produto chamado xerogel (BAETENS; JELLE; GUSTAVSEN, 2011; KHAJEH; LAURENT; DASTAFKAN, 2013; NAKAGAITO; KONDO; TAKAGI, 2013). Os xerogéis (Figura 5) possuem características químicas semelhantes aos aerogéis porém com características físicas diferentes, por exemplo a área superficial (BŁASZCZYŃSKI; ŚLOSARCZYK; MORAWSKI, 2013). Os xerogéis podem ser utilizados como suporte de catalisadores (BAILON-GARCIA et al., 2017), em processos de separação e purificação de águas residuais (ÁLVAREZ et al., 2015), células combustíveis (JOB et al., 2015) e aplicações medicinais (MUSSKAYA et al., 2011).

Figura 5 – Aerogel e xerogel produzidos com nanofibrilas de celulose.

Fonte: Do autor (2017).

Os nanofilmes são produzidos quando as nanofibrilas de celulose que estão em suspensão de depositam. As nanofibrilas se organizam em camadas (QING et al., 2015) e não podem ser dispersas novamente em água devido à grande quantidade de ligações de hidrogênio que se formam entre as nanofibrilas de celulose (NECHYPORCHUK; BELGACEM; BRAS, 2016). Os filmes produzidos são recicláveis, leves, flexíveis e com pequenos poros, podendo ser utilizados em eletrônicos, embalagens, instrumentos óticos, dentre outros (BRINCHI et al., 2013; GONZÁLEZ et al., 2014; NECHYPORCHUK; BELGACEM; BRAS, 2016; UMMARTYOTIN; MANUSPIYA, 2015b). Existem diversos métodos de preparo dos filmes e os procedimentos utilizados influenciam na resistência, opacidade, homogeneidade e

permeabilidade dos filmes. Um dos métodos é o *casting* em que o solvente da suspensão evapora naturalmente ou sob baixas temperaturas. Outro método é a filtração que pode ser feita usando membranas sob pressão ou por gravidade. A resistência mecânica dos filmes está relacionada com o grau de polimerização das nanofibrilas de celulose e a porosidade, que afeta também as propriedades de barreira por causa das alterações na permeabilidade ao vapor (HOENG; DENNEULIN; BRAS, 2016; KARKI et al., 2016; QING et al., 2015).

1.3 Quitosana

A quitosana é um biopolímero e tem sido muito utilizada no desenvolvimento de novos materiais, na forma pura ou associada com outros polímeros e materiais inorgânicos (LARANJEIRA; DE FÁVERE, 2009; LEE; CHEN; DEN, 2015; THAKUR; VOICU, 2016). A quitosana é o segundo polímero natural mais abundante (a celulose é o primeiro) e é obtida a partir da quitina (Figura 6) que é uma componente estrutural, encontrada em exoesqueletos de artrópodes ou nas paredes celulares de fungos e leveduras, e que está ordenada em microfibrilas cristalinas (ABDUL KHALIL et al., 2016; CHOI; NAM; NAH, 2015; YOUNES; RINAUDO, 2015). Existem diversos benefícios na utilização da quitosana pois é um material renovável, biodegradável, biocompatível, não tóxico, quimicamente estável e de baixo custo (DASH et al., 2011; LEE; CHEN; DEN, 2015; YOUNES; RINAUDO, 2015).

A quitina é um copolímero composto por unidades de 2-acetamida-2-desoxi-D-glucopiranose e 2-amino-2-desoxi-D-glucopiranose associadas por ligações glicosídicas β-1,4, em um arranjo linear e cristalino, e sua desacetilação em meio alcalino produz a quitosana, onde os grupos acetoamido (-$NHCOCH_3$) são convertidos em grupos amino (NH_2) (ABDUL KHALIL et al., 2016; CHOI; NAM; NAH, 2015; YOUNES; RINAUDO, 2015). A desacetilação ocorre em graus variados e depende do processo e da origem da quitina. A quitina forma ligações de hidrogênio entre cadeias devido aos grupos amina e hidroxila apresentando uma estrutura rígida e sendo insolúvel em meio aquoso e na maioria dos solventes orgânicos, porém a quitosana pode se dissolver em soluções de ácidos fracos (ácido acético, por exemplo) por causa da protonação dos grupos NH_2 (ABDUL KHALIL et al., 2016; DASH et al., 2011; THAKUR; VOICU, 2016).

Figura 6 – Estrutura da quitina e da quitosana.

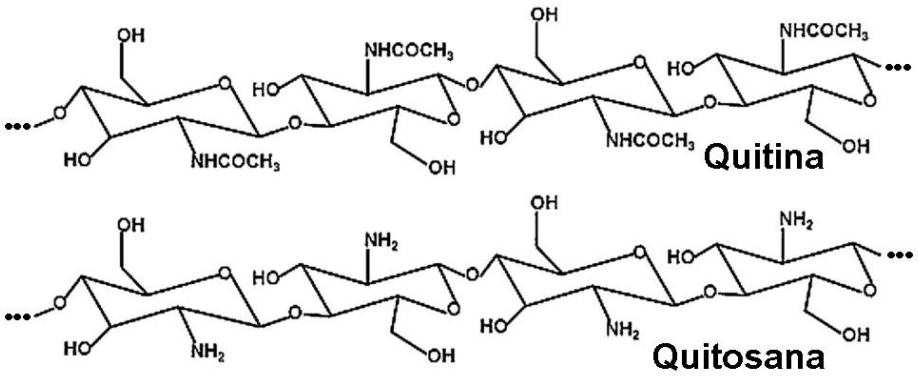

A partir da quitosana podem ser preparados diversos materiais como filmes, membranas, estruturas de liberação controlada, esponjas, pós, dentre outros, para serem utilizados na biotecnologia, biomedicina, alimentos, fármacos, catálise e aplicações ambientais (LEE; CHEN; DEN, 2015; LIU et al., 2016; THAKUR; VOICU, 2016; VAKILI et al., 2014; YOUNES; RINAUDO, 2015). Os filmes de quitosana podem ser produzidos da mesma maneira que os nanofilmes de celulose sendo muito comum o método *casting* de uma solução de quitosana em meio ácido (ABDUL KHALIL et al., 2016). Podem ser produzidos filmes somente com quitosana ou em associação com outros polímeros, como a celulose (HASSAN et al., 2016). Os filmes de quitosana- celulose apresentam características interessantes devido à similaridade estrutural dos dois polímeros podendo realizar modificações na resistência mecânica, hidrofilicidade e permeabilidade dos filmes. Os filmes são muito utilizados para embalagens (HASSAN et al., 2016), membranas de purificação de água (THAKUR; VOICU, 2016), tratamento de efluentes (ZHU et al., 2016) e aplicações elétricas (SHEN et al., 2016).

1.4 Magnetita

Os óxidos de ferro são compostos utilizados há muito tempo nas mais diversas áreas como mineralogia, medicina, biologia, geologia e química e são comumente encontrados na natureza e facilmente sintetizados em laboratório (CORNELL; SCHWERTMANN, 2003; UNSOY et al., 2015; VODYANITSKII, 2013).

Um importante óxido de ferro é a magnetita, um mineral de fórmula molecular básica Fe_3O_4, contendo Fe^{2+} e Fe^{3+}, de coloração preta e magnético. Naturalmente é encontrada em

rochas e em alguns organismos vivos e pode ser sintetizada utilizando sais de ferro (SCHWERTMANN; CORNELL, 2000; UNSOY et al., 2015). A maioria dos óxidos possuem estrutura cristalina e a magnetita apresenta cristais cúbicos com camadas de octaedros e tetraedros intercalados (Figura 7).

Figura 7 – Estrutura da magnetita alternando camadas de octaedros e tetraedros.

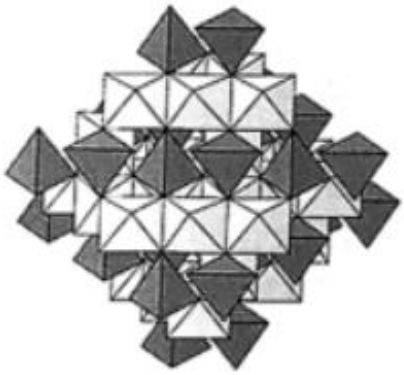

Fonte: Cornell e Schwertmann (2003).

Os óxidos de ferro podem ser utilizados como pigmentos (GOMES et al., 2013), na medicina (UNSOY et al., 2015), eletrônica (DA SILVA et al., 2017) e extensivamente na catálise (BAGHERI; JULKAPLI, 2016; SU, 2017). As aplicações catalíticas e eletrônicas geralmente necessitam de uma área superficial elevada dos materiais, o que não é característica dos óxidos de ferro, por isso, existem diversos estudos que suportam os óxidos em matrizes orgânicas, por exemplo em polímeros, para aumentar a área superficial e consequentemente aumentar a possibilidade de utilização dos materiais (PANG; KHOH; CHIN, 2011; SU, 2017). Catalisadores e filmes finos híbridos contendo magnetita e outros compostos como a celulose e a quitosana, apresentam boa estabilidade química e ampla aplicabilidade (SU, 2017).

1.5 Aplicações ambientais

Os impactos ambientais gerados pela produção industrial são frequentes e cada vez maiores e a busca por tecnologias que reduzam esses impactos, seja na diminuição da geração de resíduos ou no tratamento dos resíduos gerados, é de grande importância. As indústrias têxtil e de equipamentos eletroeletrônicos são exemplos de setores que geram uma grande quantidade

de resíduos que necessitam de tratamento e correta disposição para atender as legislações ambientais (TANSEL, 2017; WANG et al., 2016).

O setor têxtil movimenta anualmente bilhões de dólares em todo o mundo e segundo a Associação Brasileira da Indústria Têxtil (ABIT) é o segundo setor que mais emprega na indústria de transformação no país. O Brasil ocupa a quarta posição entre os maiores produtores mundiais de artigos de vestuário e a quinta posição entre os maiores produtores de manufaturas têxteis (FIEMG, 2014). O processo produtivo do setor têxtil inclui as etapas de obtenção das fibras, fiação, tecelagem, beneficiamento, acabamento, lavanderia e confecção. Durante todas as etapas são gerados resíduos, em sua maioria efluentes líquidos, com grande geração de impactos ambientais. A natureza do efluente depende do processo utilizado, mas a maioria contém uma carga elevada de matéria orgânica (BUTHIYAPPAN; ABDUL AZIZ; WAN DAUD, 2016). Para se adequar às legislações (IBAMA, SISEMA, CONAMA) as indústrias devem realizar um tratamento desses efluentes. Uma boa alternativa é a degradação catalítica de matéria orgânica via processo Fenton que pode ser feita utilizando materiais híbridos como catalisadores (ver item 1.5.1) (FIEMG, 2014; WANG et al., 2016).

A indústria eletroeletrônica cresceu exponencialmente nos últimos 50 anos, e consequentemente, a geração de resíduos eletroeletrônicos (conhecidos como e-resíduos), tornou-se uma preocupação global em termos de impactos ambientais (TANSEL, 2017; ZENG et al., 2017). Em 2015, a produção de e-resíduos girou em torno de 43 milhões de toneladas e estima-se que esse valor chegue a 50 milhões de toneladas em 2018. Esses resíduos contêm grande quantidade de materiais tóxicos e não são biodegradáveis (TANSEL, 2017). Muitos estudos para tratamento desses e-resíduos estão sendo realizados, porém uma alternativa para diminuir esse impacto ambiental é utilizar materiais renováveis e atóxicos na produção dos eletroeletrônicos, como exemplo, os materiais híbridos renováveis (ver item 1.5.2) (ZENG et al., 2017).

1.5.1 Catálise

Os processos oxidativos avançados (POA) são procedimentos catalíticos baseados na degradação de compostos orgânicos utilizando radicais (espécies altamente reativas), e são reações simples de serem realizadas e não seletivas, podendo degradar uma grande variedade de moléculas em dióxido de carbono, água e sais inorgânicos, em caso de completa mineralização (NIDHEESH; GANDHIMATHI; RAMESH, 2013; WANG et al., 2016). Um

radical bastante utilizado é a hidroxila, devido ao seu alto potencial de oxidação, e pode ser obtido a partir de oxidantes fortes, como o peróxido de hidrogênio. Quando a geração dos radicais é catalisada por íons ferro (Fe^{2+} e Fe^{3+}) o processo é conhecido como tipo Fenton (NOGUEIRA et al., 2007). Os íons ferro podem ser provenientes de sais de ferro, ferro zero ou óxidos de ferro, como a magnetita, que contem íons Fe^{2+} e Fe^{3+} na sua estrutura (BUTHIYAPPAN; ABDUL AZIZ; WAN DAUD, 2016; NIDHEESH; GANDHIMATHI; RAMESH, 2013).

O processo Fenton pode ser homogêneo ou heterogêneo. No processo homogêneo os íons ferro estão em solução e a geração dos radicais depende do pH e da concentração dos reagentes sendo necessário um pré tratamento do efluente para utilização do Fenton homogêneo (NOGUEIRA et al., 2007). Além disso, ocorre uma grande geração de lodo proveniente da deposição do ferro junto com os contaminantes que foram degradados, não sendo possível reutilizar o catalisador e sendo necessário um custo adicional para descarte desse lodo.

Uma alternativa para esses problemas é o Fenton heterogêneo cujos íons ferro estão suportados em uma matriz (híbridos) não sendo necessário o controle de pH e o catalisador pode ser reutilizado por diversos ciclos. Diversas matrizes podem ser utilizadas para suportar os íons ferro, como zeólitas, nanotubos de carbono, argilas e os biopolímeros, como a celulose (BUTHIYAPPAN; ABDUL AZIZ; WAN DAUD, 2016).

O processo Fenton é muito estudado e relatado para tratamento de efluentes têxteis que contêm alta carga de contaminantes orgânicos. Buthiyappan e colaboradores (2016) publicaram uma excelente revisão sobre os avanços e perspectivas dos processos oxidativos avançados para tratamento de efluentes têxteis e concluíram o potencial desses processos, incluindo o processo Fenton. Outra revisão de Wang e colaboradores (2016) apresenta o processo Fenton no tratamento de efluentes com alta carga de contaminantes orgânicos, e também concluem o potencial da técnica.

1.5.2 Eletrônicos

Os produtos elétricos e eletrônicos fazem parte de mercados globais com um crescimento acelerado devido ao avanço das telecomunicações e das tecnologias da informação. Muitas áreas estão envolvidas como armazenamento e transmissão de dados, gerenciamento de informações, desenvolvimento de dispositivos, entre outras que requerem baterias e armazenamento de cargas (TANSEL, 2017; ZENG et al., 2017). Os capacitores são dispositivos

compostos por duas placas condutoras paralelas contendo um material isolante entre elas, chamado de dielétrico que armazena carga após aplicação de uma tensão entre as placas (KÖTZ; CARLEN, 2000). Estão presentes em diversos dispositivos como computadores, televisores e câmeras fotográficas e são usados, por exemplo, para filtrar a passagem das correntes contínuas e alternadas, limitar interferências e suavizar as saídas de tensão (CHEN et al., 2015; NISHINO, 1996).

A capacitância (C), medida em Farads (F) é a capacidade de armazenar carga de um capacitor e é definida pela razão entre a carga armazenada (Q) no material dielétrico e a tensão aplicada entre as placas condutoras (V), ou seja, C= Q/V. A capacitância é definida pelo material dielétrico (constante dielétrica) utilizado no capacitor e esses dielétricos podem ser gasosos, sólidos ou líquidos (NISHINO, 1996).

Novos materiais têm sido estudados para serem utilizados como dielétricos visando a diminuição da geração de resíduos de difícil tratamento da indústria eletroeletrônica. Os materiais híbridos renováveis e biodegradáveis, compostos de celulose, quitosana e óxidos de ferro se apresentam como uma alternativa para serem utilizados nos chamados eletrônicos verdes (DA SILVA et al., 2017; PETRITZ et al., 2013; VELLAKKAT; HUNDEKAL, 2017).

REFERÊNCIAS

ABDUL KHALIL, H. P. S. et al. Production and modification of nanofibrillated cellulose using various mechanical processes: A review. **Carbohydrate Polymers**, London, v. 99, p. 649–665, 2014.

ABDUL KHALIL, H. P. S. et al. A review on chitosan-cellulose blends and nanocellulose reinforced chitosan biocomposites: Properties and their applications. **Carbohydrate Polymers**, v. 150, p. 216–226, 2016.

ABDUL KHALIL, H. P. S.; BHAT, A. H.; IREANA YUSRA, A. F. Green composites from sustainable cellulose nanofibrils: A review. **Carbohydrate Polymers**, v. 87, n. 2, p. 963–979, jan. 2012.

ALHASSEN, H. et al. Organic/Hybrid Nanoparticles and Single-Walled Carbon Nanotubes: Preparation Methods and Chiral Applications. **Chirality**, v. 26, n. 11, p. 683–691, nov. 2014.

ÁLVAREZ, S. et al. Synthesis of carbon xerogels and their application in adsorption studies of caffeine and diclofenac as emerging contaminants. **Chemical Engineering Research and Design**, v. 95, p. 229–238, 2015.

BAETENS, R.; JELLE, B. P.; GUSTAVSEN, A. Aerogel insulation for building applications: A state-of-the-art review. **Energy and Buildings**, v. 43, n. 4, p. 761–769, abr. 2011.

BAGHERI, S.; JULKAPLI, N. M. Modified iron oxide nanomaterials: Functionalization and application. **Journal of Magnetism and Magnetic Materials**, v. 416, p. 117–133, 2016.

BAILON-GARCIA, E. et al. New carbon xerogel-TiO2 composites with high performance as visible-light photocatalysts for dye mineralization. **Applied Catalysis B: Environmental**, v. 201, p. 29–40, 2017.

BARNETT, J. R.; JERONIMIDIS, G. **Wood Quality and its Biological Basis**. Flórida: Blackwell Publishing, 2003.

BŁASZCZYŃSKI, T.; ŚLOSARCZYK, A.; MORAWSKI, M. Synthesis of Silica Aerogel by Supercritical Drying Method. **Procedia Engineering**, v. 57, n. October 2015, p. 200–206, 2013.

BOUFI, S. et al. Nanofibrillated cellulose as an additive in papermaking process: A review. **Carbohydrate Polymers**, v. 154, p. 151–166, 2016.

BRINCHI, L. et al. Production of nanocrystalline cellulose from lignocellulosic biomass: Technology and applications. **Carbohydrate Polymers**, v. 94, n. 1, p. 154–169, 2013.

BURTON, R. A; GIDLEY, M. J.; FINCHER, G. B. Heterogeneity in the chemistry, structure and function of plant cell walls. **Nature chemical biology**, v. 6, n. 10, p. 724–32, out. 2010.

BUTHIYAPPAN, A.; ABDUL AZIZ, A. R.; WAN DAUD, W. M. A. Recent advances and prospects of catalytic advanced oxidation process in treating textile effluents. **Reviews in Chemical Engineering**, v. 32, n. 1, p. 1–47, 2016.

CAPOLUPO, L.; FARACO, V. Green methods of lignocellulose pretreatment for biorefinery development. **Applied Microbiology and Biotechnology**, v. 100, n. 22, p. 9451–9467, 2016.

CAVALIERI, F. et al. Nanomedicines for antimicrobial interventions. **Journal of Hospital Infection**, v. 88, n. 4, p. 183–190, 2014.

CHANG, C.; ZHANG, L. Cellulose-based hydrogels: Present status and application prospects. **Carbohydrate Polymers**, v. 84, n. 1, p. 40–53, 2011.

CHEN, Q. et al. Polymer-Based Dielectrics with High Energy Storage Density. **Annu. Rev. Mater. Res**, v. 45, p. 433–58, 2015.

CHIN, S. F.; BINTI ROMAINOR, A. N.; PANG, S. C. Fabrication of hydrophobic and magnetic cellulose aerogel with high oil absorption capacity. **Materials Letters**, v. 115, p. 241–243, jan. 2014.

CHOI, C.; NAM, J. P.; NAH, J. W. Application of chitosan and chitosan derivatives as biomaterials. **Journal of Industrial and Engineering Chemistry**, v. 33, p. 1–10, 2015.

CORNELL, R. M.; SCHWERTMANN, U. **The Iron Oxides**. 2. ed. Verlag: Wiley- VCH, 2003.

DA SILVA, A. L. et al. Superparamagnetic nano-biocomposites for application as dielectric resonator antennas. **Materials Chemistry and Physics**, v. 185, p. 104–113, 2017.

DASH, M. et al. Chitosan - A versatile semi-synthetic polymer in biomedical applications. **Progress in Polymer Science (Oxford)**, v. 36, n. 8, p. 981–1014, 2011.

EK, M.; GELLERSTEDT, G.; HENRIKSSON, G. **Pulp and Paper Chemistry and Technology Volume 1**. Stockholm: Gruyter, 2009. v. 1

FENGEL, D.; WEGENER, G. **Wood: chemistry, ultrastructure, reactions**. Berlin: Walter de Gruyter, 1984.

FIEMG. **Guia técnico ambiental da indústria têxtil**. Disponível em: <www.abit.org.br>. Acesso em: 9 jan. 2017.

GOMES, H. et al. Identification of pigments used in rock art paintings in Gode Roriso-Ethiopia using Micro-Raman spectroscopy. **Journal of Archaeological Science**, v. 40, n. 11, p. 4073–4082, 2013.

GONZÁLEZ, I. et al. From paper to nanopaper: Evolution of mechanical and physical properties. **Cellulose**, v. 21, n. 4, p. 2599–2609, 2014.

HAN, S. et al. Green and facile fabrication of carbon aerogels from cellulose-based waste newspaper for solving organic pollution. **Carbohydrate Polymers**, v. 136, p. 95–100, 2016.

HASSAN, E. A. et al. Novel nanofibrillated cellulose/chitosan nanoparticles nanocomposites films and their use for paper coating. **Industrial Crops and Products**, v. 93, p. 219–226, 2016.

HOENG, F.; DENNEULIN, A.; BRAS, J. Use of nanocellulose in printed electronics: A review. **Nanoscale**, v. 8, p. 13131–13154, 2016.

JOB, N. et al. Design of Pt/Carbon Xerogel Catalysts for PEM Fuel Cells. **Catalysts**, v. 5, n. 1, p. 40–57, 2015.

JOHN, M. J.; THOMAS, S. Biofibres and biocomposites. **Carbohydrate Polymers**, v. 71, n. 3, p. 343–364, 2008.

JOSÉ, N. M.; PRADO, L. A. S. D. A. Materiais híbridos orgânico-inorgânicos: Preparação e algumas aplicações. **Quimica Nova**, v. 28, n. 2, p. 281–288, 2005.

KARKI, S. et al. Thin films as an emerging platform for drug delivery. **Asian Journal of Pharmaceutical Sciences**, v. 11, n. 5, p. 559–574, 2016.

KHAJEH, M.; LAURENT, S.; DASTAFKAN, K. Nanoadsorbents: classification, preparation, and applications (with emphasis on aqueous media). **Chemical reviews**, v. 113, n. 10, p. 7728–68, 9 out. 2013.

KISTLER, S. S. Coherent Expanded Aerogels and Jellies. **Nature**, v. 127, n. 3211, p. 741, 1931.

KO, Y. G.; CHOI, U. S. Diverse applications of fibers surface-functionalized with nano- and microparticles. **Composites Science and Technology**, v. 79, p. 77–86, 2013.

KÖTZ, R.; CARLEN, M. Principles and applications of electrochemical capacitors. **Electrochimica Acta**, v. 45, n. 15, p. 2483–2498, 2000.

KUMAR, P. et al. Methods for Pretreatment of Lignocellulosic Biomass for Efficient Hydrolysis and Biofuel Production. **Ind. Eng. Chem. Res.**, v. 48, n. 8, p. 3713–3729, 2009.

LARANJEIRA, M. C. M.; DE FÁVERE, V. T. Quitosana: biopolimero funcional com potencial industrial biomedico. **Quimica Nova**, v. 32, n. 3, p. 672–678, 2009.

LAVOINE, N. et al. Microfibrillated cellulose - Its barrier properties and applications in cellulosic materials: A review. **Carbohydrate Polymers**, v. 90, n. 2, p. 735–764, 2012.

LEE, K. Y. et al. On the use of nanocellulose as reinforcement in polymer matrix composites. **Composites Science and Technology**, v. 105, p. 15–27, 2014.

LEE, M.; CHEN, B.-Y.; DEN, W. Chitosan as a Natural Polymer for Heterogeneous Catalysts Support: A Short Review on Its Applications. **Applied Sciences**, v. 5, n. 4, p. 1272–1283, 2015.

LIU, Y. et al. Mechanical and water vapor barrier properties of bagasse hemicellulose-based films. **BioResources**, v. 11, n. 2, p. 4226–4236, 2016.

MALUCELLI, G. et al. Materials engineering for surface-confined flame retardancy. **Materials Science and Engineering R: Reports**, v. 84, n. 1, p. 1–20, 2014.

MULYADI, A.; ZHANG, Z.; DENG, Y. Fluorine-Free Oil Absorbents Made from Cellulose Nanofibril Aerogels. **ACS Applied Materials & Interfaces**, v. 8, p. 2732–2740, 2016.

MUSSKAYA, O. N. et al. Nanocomposite biomaterials based on hydroxyapatite xerogel. **Glass Physics and Chemistry**, v. 37, n. 5, p. 525–532, 2011.

NAKAGAITO, A.; KONDO, H.; TAKAGI, H. Cellulose nanofiber aerogel production and applications. **Journal of Reinforced Plastics and Composites**, v. 32, n. 20, p. 1547–1552, 20 jun. 2013.

NECHYPORCHUK, O.; BELGACEM, M. N.; BRAS, J. Production of cellulose nanofibrils: A review of recent advances. **Industrial Crops and Products**, v. 93, p. 2–25, 2016.

NIDHEESH, P. V.; GANDHIMATHI, R.; RAMESH, S. T. Degradation of dyes from aqueous solution by Fenton processes: A review. **Environmental Science and Pollution Research**, v. 20, n. 4, p. 2099–2132, 2013.

NISHINO, A. Capacitors: operating principles, current market and technical trends. **Journal of Power Sources**, v. 60, n. 2, p. 137–147, 1996.

NOGUEIRA, R. F. P. et al. Fundaments and environmental applications of Fenton and Photo-Fenton processes. **Quimica Nova**, v. 30, n. 2, p. 400–408, 2007.

PANG, S. C.; KHOH, W. H.; CHIN, S. F. Synthesis and Characterization of Magnetite/Carbon Nanocomposite Thin Films for Electrochemical Applications. **Journal of Materials Science & Technology**, v. 27, n. 10, p. 873–878, 2011.

PANZELLA, L. et al. Surface-Functionalization of Nanostructured Cellulose Aerogels by Solid State Eumelanin Coating. **Biomacromolecules**, v. 17, n. 2, p. 564–571, fev. 2016.

PETRITZ, A. et al. Cellulose as biodegradable high-k dielectric layer in organic complementary inverters. **Applied Physics Letters**, v. 103, n. 15, 2013.

QING, Y. et al. Self-assembled optically transparent cellulose nanofibril films: effect of

nanofibril morphology and drying procedure. **Cellulose**, v. 22, n. 2, p. 1091–1102, 2015.

RATH, K. Novel Materials from Solgel Chemistry. **Science & Technology Review**, v. 4, n. 1, p. 24–26, maio 2005.

SALAS, C. et al. Nanocellulose properties and applications in colloids and interfaces. **Current Opinion in Colloid and Interface Science**, v. 19, n. 5, p. 383–396, 2014.

SARKAR, N. et al. Bioethanol production from agricultural wastes: An overview. **Renewable Energy**, v. 37, p. 19–27, jul. 2011.

SCHWERTMANN, U.; CORNELL, R. M. **Iron Oxides in the Laboratory**. Second ed. Verlag: Wiley- VCH, 2000.

SHEN, X. et al. Hydrogels Based on Cellulose and Chitin: Fabrication, Properties, and Applications. **Green Chemistry**, v. 18, p. 53–75, 2016.

SINGH, R. et al. A review on delignification of lignocellulosic biomass for enhancement of ethanol production potential. **Renewable and Sustainable Energy Reviews**, v. 32, p. 713–728, 2014.

SMALL, A. C.; JOHNSTON, J. H. Novel hybrid materials of magnetic nanoparticles and cellulose fibers. **Journal of Colloid and Interface Science**, v. 331, n. 1, p. 122–126, 2009.

SU, C. Environmental implications and applications of engineered nanoscale magnetite and its hybrid nanocomposites: A review of recent literature. **Journal of Hazardous Materials**, v. 322, p. 48–84, 2017.

TAN, X. FEI et al. Biochar-based nano-composites for the decontamination of wastewater: A review. **Bioresource Technology**, v. 212, p. 318–333, 2016.

TANSEL, B. From electronic consumer products to e-wastes: Global outlook, waste quantities, recycling challenges. **Environment International**, v. 98, p. 35–45, 2017.

THAKUR, V. K.; VOICU, S. I. Recent advances in cellulose and chitosan based membranes for water purification: A concise review. **Carbohydrate Polymers**, v. 146, p. 148–165, 2016.

TONOLI, G. H. D. et al. Properties of cellulose micro/nanofibers obtained from eucalyptus pulp fiber treated with anaerobic digestate and high shear mixing. **Cellulose**, v. 23, p. 1239–1256, 2016.

TRACHE, D. et al. Microcrystalline cellulose: Isolation, characterization and bio-composites application - A review. **International Journal of Biological Macromolecules**, v. 93, p. 789–804, 2016.

UMMARTYOTIN, S.; MANUSPIYA, H. A critical review on cellulose: From fundamental to an approach on sensor technology. **Renewable and Sustainable Energy Reviews**, v. 41, p. 402–412, 2015a.

UMMARTYOTIN, S.; MANUSPIYA, H. An overview of feasibilities and challenge of conductive cellulose for rechargeable lithium based battery. **Renewable and Sustainable Energy Reviews**, v. 50, p. 204–213, 2015b.

UNSOY, G. et al. Magnetite: From synthesis to applications. **Current Topics in Medicinal Chemistry**, v. 15, n. 16, p. 1622–1640, 2015.

VAKILI, M. et al. Application of chitosan and its derivatives as adsorbents for dye removal from water and wastewater: A review. **Carbohydrate Polymers**, v. 113, p. 115–130, 2014.

VELLAKKAT, M.; HUNDEKAL, D. Electrical conductivity and supercapacitor properties of

polyaniline/chitosan/nickel oxide honeycomb nanocomposite. **Journal of Applied Polymer Science**, v. 134, n. 9, p. 1–12, 2017.

VODYANITSKII, Y. N. Biogeochemical role of magnetite in urban soils (Review of publications). **Eurasian Soil Science**, v. 46, n. 3, p. 317–324, 27 mar. 2013.

WAN, C. et al. Cellulose aerogels from cellulose–NaOH/PEG solution and comparison with different cellulose contents. **Materials Science and Technology**, v. 31, n. 9, p. 1096–1102, 2015.

WAN, C.; LI, J. Synthesis of well-dispersed magnetic CoFe2O4 nanoparticles in cellulose aerogels via a facile oxidative co-precipitation method. **Carbohydrate Polymers**, v. 134, p. 144–150, 2015.

WANG, N. et al. A review on Fenton-like processes for organic wastewater treatment. **Journal of Environmental Chemical Engineering**, v. 4, n. 1, p. 762–787, 2016.

WANG, S.; LU, A.; ZHANG, L. Recent advances in regenerated cellulose materials. **Progress in Polymer Science**, v. 53, p. 169–206, 2016.

YANG, J. et al. Cellulose/graphene aerogel supported phase change composites with high thermal conductivity and good shape stability for thermal energy storage. **Carbon**, v. 98, p. 50–57, 2016.

YOUNES, I.; RINAUDO, M. Chitin and chitosan preparation from marine sources. Structure, properties and applications. **Marine Drugs**, v. 13, n. 3, p. 1133–1174, 2015.

ZENG, X. et al. Innovating e-waste management: From macroscopic to microscopic scales. **Science of the Total Environment**, v. 575, p. 1–5, 2017.

ZHANG, X. et al. Solid-state flexible polyaniline/silver cellulose nanofibrils aerogel supercapacitors. **Journal of Power Sources**, v. 246, p. 283–289, jan. 2014.

ZHOU, Z. et al. Polyaniline-decorated cellulose aerogel nanocomposite with strong interfacial adhesion and enhanced photocatalytic activity. **RSC Advances**, v. 4, n. 18, p. 8966, 2014.

ZHU, X. et al. Removal of toxic indigo blue with integrated biomaterials of sodium carboxymethyl cellulose and chitosan. **International Journal of Biological Macromolecules**, v. 91, p. 409–415, 2016.

ZUGENMAIER, P. **Crystalline Cellulose and Derivatives**. 1. ed. Berlin: Springer, 2008. 295 p.

SEGUNDA PARTE

ARTIGO 1

Renewable hybrid nanocatalyst from magnetite and cellulose for treatment of textile effluents

Artigo aceito para publicação na revista "Carbohydrate Polymers"

Fator de impacto: 4.689

Classificação Ciências Agrárias I: A1

DOI: 10.1016/j.carbpol.2017.01.007

Ana Carolina Cunha Arantes[1], Crislaine das Graças Almeida[1], Ligiane Carolina Leite Dauzacker[1], Maria Lucia Bianchi[1], Delilah F. Wood[2], Tina G. Williams[2], William J. Orts[2], Gustavo Henrique Denzin Tonoli[3]

[1] Department of Chemistry, Federal University of Lavras, CP 3037, Lavras- MG, Brazil.
[2] Bioproducts Research Unit, WRRC, ARS- USDA, 800 Buchanan St., Albany, CA 94710, USA.
[3] Department of Forest Sciences, Federal University of Lavras, CP 3037, Lavras- MG, Brazil.

Abstract

In this study, a hybrid catalyst was prepared using cellulose nanofibrils and magnetite to degrade organic compounds. Cellulose nanofibrils were isolated by mechanical defibrillation producing a suspension used as a matrix for magnetite particles. The solution of nanofibrils and magnetite was dried and milled resulting in a catalyst with a 1:1 ratio of cellulose and magnetite that was chemically and physically characterized using light, scanning electron and transmission electron microscopies, specific surface area analysis, vibrating sample magnetometry, thermogravimetric analysis, Fourier transform infrared spectroscopy, X-ray diffraction, catalytic potential and degradation kinetics. Results showed good dispersion of the active phase, magnetite, in the mat of cellulosic nanofibrils. Leaching and re-use tests showed that catalytic activity was not lost over several cycles. The hybrid material produced was tested for degradation of methylene blue dye in Fenton-like reactions resulting in a potential catalyst for use in degradation of organic compounds.

Keywords: magnetite, catalyst, cellulose, nanofibrils, crystallite.

1. Introduction

Cellulose has been studied and applied as a precursor of new bioengineered materials (Oksman et al., 2016; Reza et al., 2015; Zhu, Ma, Li, Pan, & Dai, 2015) and is organized at a macromolecular level into fibrils consisting of glucose units in a linear and crystalline arrangement, along with hemicellulose and lignin (Fengel & Wegener, 1984; Zugenmaier, 2008). Cellulose fibers are made up of basic crystalline building-blocks or nanofibrils that can form suspensions in water when isolated (Chen et al., 2014).

The isolation process, typically by chemical or physical methods, can affect the properties of the resulting cellulose nanofibrils (Wang, Li, Yano, & Abe, 2014). Mechanical defibrillation is a physical process where cellulose fibers pass through a mill that reduces their dimensions by friction. At a certain size range, the nanofibrils form a gel-like suspension (Bufalino et al., 2015; Fonseca et al., 2016). Defibrillation is a physical method that requires no chemicals in the isolation of cellulose nanofibrils, thus, reduces processing steps and pollution.

Cellulose nanofibrils can be used to prepare a multitude of useful commercial materials, such as aerogels, xerogels, hydrogels, beads and specialty biomaterials (including medical grafts) (Abe & Yano, 2011; Baetens, Jelle, & Gustavsen, 2011; Chin, Binti Romainor, & Pang, 2014; Eichhorn et al., 2010; Gericke, Trygg, & Fardim, 2013; Wan & Li, 2015). Aerogels have low density, high strength and a large surface area (Innerlohinger, Weber, & Kraft, 2006) and are produced by supercritical drying of cellulose nanofiber suspensions which allows them to maintain a structured gel (Heath & Thielemans, 2010). Air drying of nanofiber suspensions causes the gel structure to collapse resulting in a xerogel (Baetens et al., 2011). Depending on the final application, a xerogel may have the same benefits of an aerogel without the high costs of supercritical drying.

Aerogels and xerogels made from cellulose can serve as fixed supports for Fe ions in the production of chemical catalysts (Small & Johnston, 2009). These Fe-hybridized aerogels can be expected to be used in a number of industrial applications as they have superparamagnetic properties, remarkable mechanical strength, are lightweight, flexible, highly porous and have a large surface area that provide a huge number of reactive sites (Liu, Yan, Tao, Yu, & Liu, 2012). In addition to being produced from readily renewable resources, such as wheat straw, an agricultural residue, aerogels may be prepared using green chemical methods which further extends their usefulness and acceptability as a green product (Wan & Li, 2015). Olsson and coworkers used highly flexible and porous hybrid aerogels as templates to construct

solid and stiff nanocomposites by compaction (Olsson et al., 2010). Fe ions may be used to catalyze Fenton-like reactions for the generation of hydroxyl radicals using strong oxidizing agents, such as H_2O_2, as a precursor. Hydroxyl radicals have high oxidation potential and can degrade organic molecules, such as dyes generated in textile effluents (Nogueira, Trovó, Da Silva, Villa, & De Oliveira, 2007).

The use of iron-based catalyst systems is advantageous because iron is a naturally-occurring, abundant compound that is non-toxic, environmentally safe and readily renewable and sustainable. Some forms of iron oxide have magnetic properties facilitating the removal of reactants so that they can be readily reused (Luo & Zhang, 2009). Magnetite, a dark colored iron oxide, with the molecular formula Fe_3O_4, provides magnetic properties to materials and supplies Fe ions to catalyze Fenton- like reactions.

The aim of this study was to evaluate the catalytic efficiency of a magnetic catalyst produced by impregnating cellulose nanofibrils with magnetite and applied to the degradation of methylene blue dye in a Fenton-like reactive process.

2. Materials and methods

2.1. Production and characterization of the cellulose suspension

The fibers of commercial eucalyptus kraft pulp (Jacareí/SP, Brazil) were immersed in distilled water for 48 h at 1% (w/w) concentration before defibrillation. Cellulose nanofibrils were obtained by mechanical defibrillation of the fiber cell wall using a SuperMasscolloider MKCA6-3 , (Masuko Sangyo Co., LTD, Japan), operated at 1500 rpm, with a 0.01 mm opening between disks and applying 35 passages through the defibrillator (Bufalino et al., 2015; Tonoli et al., 2016). The resulting nanofibril suspensions were characterized morphologically using a Nikon Eclipse E200 (Japan) compound microscope by randomly selecting 10 areas on a slide for image analysis. Glass slides were prepared with 0.05 mL of sample mounted in glycerin.

Scanning electron microscopy (SEM) was performed using a Hitachi S4700 field emission SEM (Hitachi High-Technologies, Japan). The freeze-dried samples were adhered to aluminum specimen stubs using double-sided adhesive-coated carbon tabs (Ted Pella, Inc., Redding, CA). The samples were then sputter-coated with gold-palladium in a Denton Desk II sputter coating unit (Moorestown, NJ). SEM images were captured at a resolution of 2650x1920 pixels.

Transmission electron microscopy (TEM) was used to visualize the cellulose nanofibrils by mixing the suspended samples with uranyl acetate to make the cellulose particles electron dense in order to provide contrast in the TEM. A drop of the nanofibril suspension was placed onto a 400-mesh carbon-formvar grid (Ted Pella, Inc., Redding, CA) held at the edge of with double-adhesive tape. The grids were allowed to air-dry and then were observed and photographed in a FEI Tecnai 12 TEM (FEI Company, Hillsboro, OR) operated at 120 kV. The average diameter of the micro/nanofibrils was determined by digital image analyses (ImageJ 1.48v, National Institutes of Health, USA) on TEM micrographs. A minimum of 100 measurements was collected for analyses.

2.2. Production and characterization of the magnetic hybrids

The synthesis of magnetic material was performed using the methodology adapted from Schwertmann & Cornell (2000). Fe^{2+} and Fe^{3+} salts (6.314 g of $FeCl_3$ and 2.343 g of $FeCl_2$) were dissolved in 200 mL of an aqueous suspension of cellulose nanofibrils under nitrogen flow. NH_4OH was added until pH 11 was attained to precipitate both magnetite and cellulose from solution. The precipitate was washed with water until pH~7, oven-dried at 60°C, and milled in a ball mill. The mass ratio of cellulose:magnetite was 1:1 (cel:mag). To obtain the ratio, the experimental sample was compared to a sample of pure magnetite (magnetite) prepared by a similar method.

Surface areas were determined via N_2 adsorption at −196 °C in an Autosorb-1 Quantachrome system (Quantachrome Instruments, Boynton Beach, FL). The samples were previously degassed at 110 °C for 10 h, and the specific area was calculated using the Brunauer-Emmett-Teller (BET) model. Magnetic properties of the materials were measured by vibrating sample magnetometry (VSM) using an ADE/DMS Model 880 Vibrating Sample Magnetometer (MicroSense, LLC, Lowell, MA). Thermogravimetric analysis (TGA) was performed using a Shimadzu DTG-60AH TGA (Shimadzu Corporation, Kyoto, Japan). Samples (approximately 10 mg) were heated under synthetic air atmosphere in the range of 25 to 800°C with a heating rate of 10°C.min^{-1} and a gas flow rate of 30 mL.min^{-1}. Fourier transform infrared spectroscopy (FTIR) was performed using a Shimadzu spectrophotometer IRAffinity system, with KBr pellets containing 1% sample, in the spectral range of 400 to 4000 cm^{-1}, 4 cm^{-1} resolution with 32 scans. X-ray diffraction (XRD) was performed using a Shimadzu XRD-6000 equipped with a graphite crystal as monochromator to collimate Cu-$K_{\alpha 1}$ radiation at λ = 1.5406 Å with a step of 0.02°.s^{-1} and an angular range (2θ) of 4° to 70°.

2.3. Catalytic tests

Assays of the catalytic decomposition of H_2O_2 by cel:mag were performed, under stirring, using 30 mg of the cel:mag catalyst, 5 mL of water and 2 mL of H_2O_2. The volume of oxygen produced was monitored by displacement of water with a column over 30 minutes of reaction. A comparative reaction was also run using 30 mg of catalyst, 5 mL of methylene blue (50 ppm) and 2 mL of H_2O_2. For leaching tests, 60 mg of the cel:mag catalyst were stirred with 10 mL of water for 180 min; then, decomposition of H_2O_2 was measured using 5 mL of the supernatant. For the dye tests, catalytic properties were assayed via kinetic degradation of methylene blue dye using 10 mg of the cel:mag catalyst, 9.9 mL of 50 ppm methylene blue solution and 0.1 mL of H_2O_2. Reactions were monitored by spectrophotometry in UV-visible at 665 nm at 0, 15, 30, 60, 90, 120 and 180 min. All tests were performed using either the cel:mag or the magnetite catalytic formulations. Moreover, the degradation kinetics were also performed for pure cellulose.

3. Results and discussion

3.1. Morphology of the cellulose nanofibrils

One feature that determines the presence of nanofibrils is the formation of an increasingly gel-like suspension with successive passages through the defibrillator (Nakagaito & Yano, 2004). When the solution containing cellulose fibers passes through the defibrillator, disintegration of the cell walls occur, thus modifying the dimensions and surface structure of the fibers. Structural modification results in viscosity changes due to the breaking and reformation of chemical bonds. The crystallinity index and degree of polymerization are also changed with consecutive passages (Uetani & Yano, 2011). Light microscopy images (Fig. 1a, 1b) present the cellulose fibers before and after passages through the defibrillator (35 cycles), and the size changes in the nanofibrils may be clearly observed. Fig. 1c shows a transmission electron micrograph (TEM) of the nanofibrils obtained by mechanical defibrillation of the starting cellulose pulp fibers. Defibrillation decreases the average fiber length significantly and increases the swelling capacity by fracturing the fibrils, resulting in a considerable increase in surface area (Tonoli, Fuente, et al., 2009; Tonoli et al., 2016; Tonoli, Rodrigues Filho, et al., 2009). High shear applied to fibers during defibrillation efficiently disintegrated fibers into small fragments and, to some extent, separated individual nanofibrils. The accumulated

nanofibril diameter distribution is presented in Fig. 1d. The average diameter of nanofibrils was 50 ± 41 nm, with roughly 55% of the nanofibrils at a diameter of less than 40 nm.

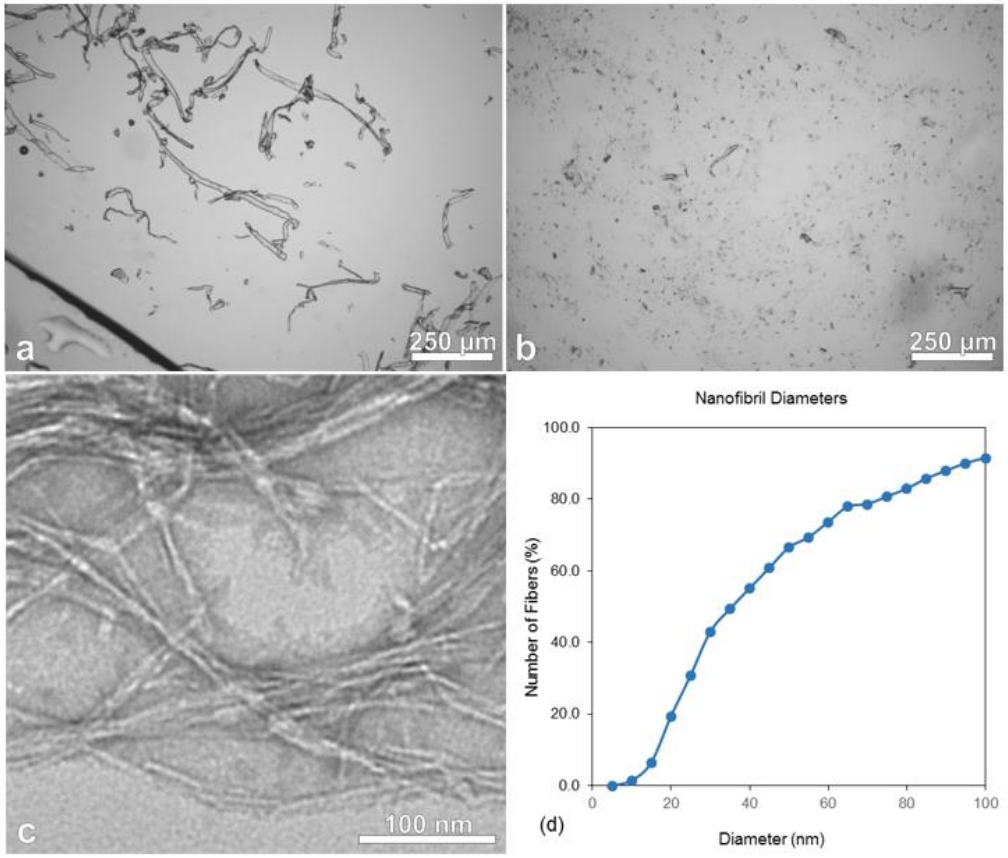

Fig. 1 Optical microscopy images of cellulose pulp fibers before defibrillation (a) and cellulose nanofibrils obtained by mechanical defibrillation of cellulose fibers (b); transmission electron microscopy (TEM) micrograph showing the nanofibrils after defibrillation (c); accumulated diameter distribution of the nanofibrils after measurements using TEM micrographs (d).

The presence of fibers larger than the nanoscale can be observed in the suspension (content larger than 100 nm in Fig. 1d), although this did not preclude formation of catalysts since the suspensions remained stable and well-dispersed with no separation of the cellulose nanofibrils (Fig. 2a). The minimization of steps in the milling protocol will reduce the production costs of catalysts, an important advantage in large-scale production. The production of catalyst with cellulose without passing through the defibrillator was also tested as a control experiment, but these cellulose fibers tended to cluster and did not form a stable suspension (Fig. 2b). Therefore, the synthesis of catalysts without defibrillation produced an inhomogeneous solution where the active phase was not well dispersed, forming magnetite clusters with long fibers of cellulose.

3.2. Properties of the hybrids magnetic materials

A homogeneous magnetic material was produced (cel:mag) that could be classified as a xerogel since its slow oven-drying would result in a loss of microporosity. The cel:mag material was milled to reduce the particle size and to increase the surface area, an important characteristic of a catalyst. The final mass yield for the synthesis was 94% resulting in a material with amphiphilic (Fig. 2c) and magnetic (Fig. 2d) properties. Both properties increase the application possibilities in different reaction media and facilitate the reuse of the material.

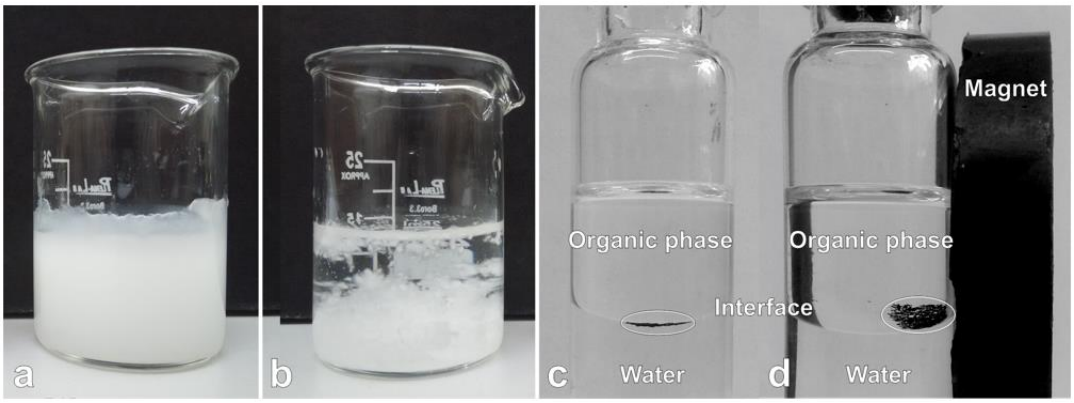

Fig. 2 Cellulose fibers after (a) and before (b) mechanical defibrillation. Note the uneven dispersion of fibers in (b) and the stable and well-dispersed suspension in (a). The amphiphilic property of the hybrid catalyst demonstrated when the catalyst remains in the interface of organic phase and aqueous mixture (c) magnetic propriety demonstrated when the hybrid catalyst is attracted by a magnet (d).

Magnetite on its own generally forms clusters in aqueous solutions leading to a loss of activity in Fenton-like processes because the surface area is reduced thereby reducing access to reactive Fe ions. To improve the efficiency of the catalyst, the magnetite was synthesized in association with cellulose nanofibrils. Nanofibrils maintain a large surface area and since cellulose does not dissolve in water or organic solvents, it was hypothesized that magnetite dispersed in cellulose would form a stable solution. Such a dispersed matrix with a large surface area would increase access to catalytic sites, thus promoting longer catalytic life.

To verify the hypothesis of an increased number of reactive sites, specific surface area analyses of the materials (cel:mag and magnetite) and the isotherms of N_2(g) adsorption-desorption were performed (Fig 3a). The isotherms present a hysteresis type IV typical of mesoporous materials shown as pore size distribution (Fig. 3a, insert) with strong adsorbent-adsorbate interactions (Thommes, et al., 2015). The specific surface areas calculated are

$30 m^2 g^{-1}$ and $112 m^2 g^{-1}$ for magnetite and cel:mag, respectively. The increase in surface area demonstrates the advantage of using magnetite on cellulose nanofibrils.

The magnetic properties were studied by performing a VSM analysis and Fig. 3b exhibits the hysteresis loop of the materials. The hysteresis and coercivity of samples are characteristic of superparamagnetic materials. The saturation magnetization of cel:mag at 29.74 emu/g is comparable to that of pure magnetite at 31.58 emu/g indicating that the cellulose matrix doesn't affect the superparamagnetic property of the magnetite.

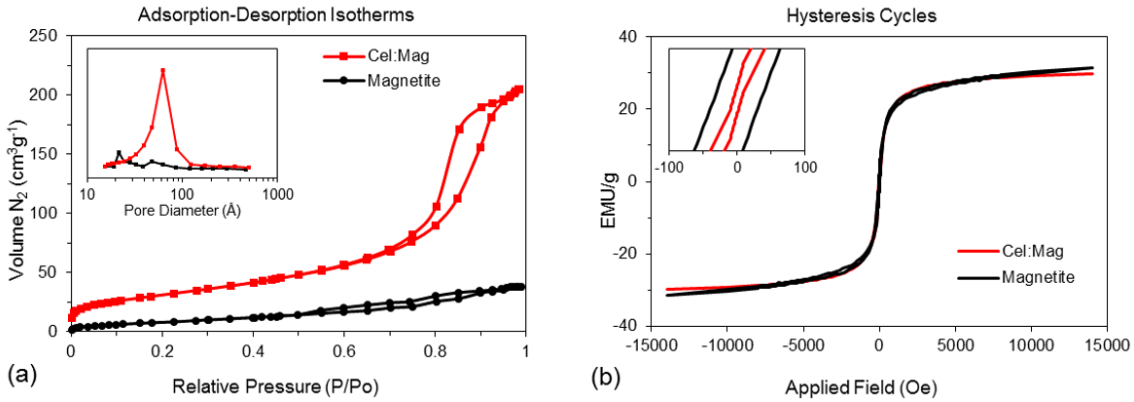

Fig. 3. (a) $N_{2(g)}$ adsorption-desorption isotherms (the insert shows the pore size distribution) and (b) hysteresis cycles (the insert shows the initial magnetization curve as a function of applied magnetic field) of the hybrid catalyst synthetized with cellulose nanofibrils and magnetite (Cel:Mag) and pure magnetite (Magnetite).

Interactions and dispersions of magnetite and cel:mag were observed via SEM and image analysis (Fig. 4). Pure magnetite forms clusters (Fig. 4a) that do not disperse in aqueous media. The cel:mag also forms clusters; however, the magnetite clusters are distributed in a web of cellulose nanofibrils (Fig. 4b). The cel:mag clusters have an increased surface area over the magnetite clusters which increases the access to catalytic sites in the cel:mag material. Since cellulose is water insoluble, the system remains stable, with materials well-dispersed in the reaction medium. Recovery of the magnetic material from the stable matrix is much faster than from the unstable matrix (magnetite alone) thus, making it much easier to re-use the nanofibril catalyst than it is to recover the pure magnetite.

TEM images also show the dispersion of magnetite within the web of cellulose nanofibrils (Fig. 4c, 4d). Cellulose does not readily stain with uranyl acetate, thus cellulose regions are less electron dense than the magnetite regions, which readily take up uranyl acetate

and become electron dense. Thus, in Fig. 4c, d, cellulose is relatively light-colored while magnetite is revealed as dark spots dispersed in the matrix.

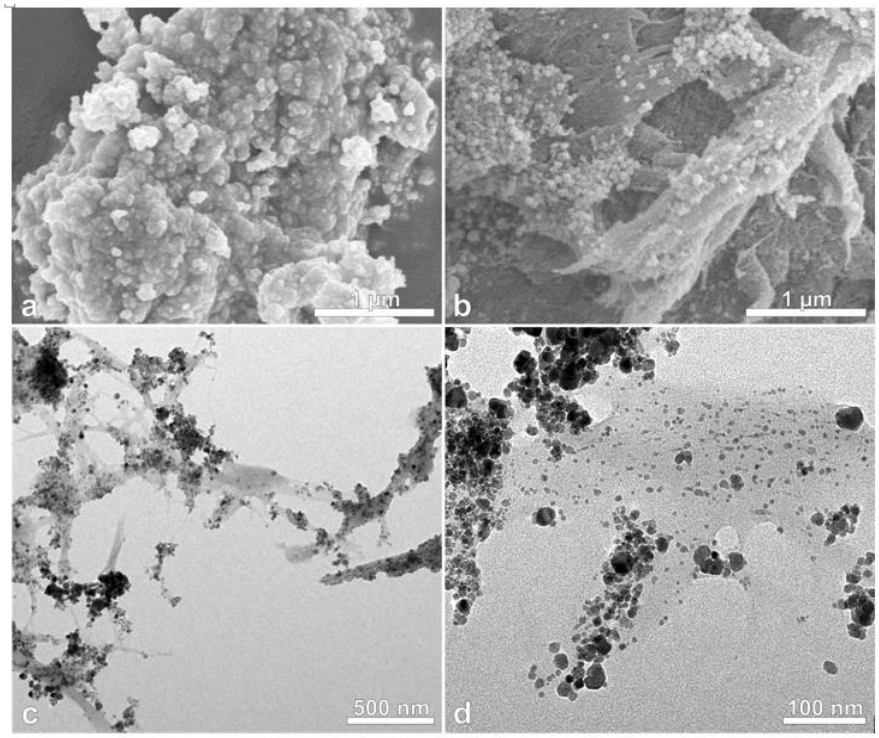

Fig. 4 Typical electron micrographs of a cluster of synthetized pure magnetite (a) and the hybrid catalyst (cel:mag) synthetized with cellulose nanofibrils and magnetite showing the magnetite dispersed into the web of the cellulose nanofibrils (b) viewed by scanning electron microscopy (SEM). The hybrid catalyst (cel:mag) synthetized with cellulose nanofibrils and magnetite showing the magnetite dispersed into the web of the cellulose nanofibrils (c, d) viewed by transmission electron microscopy (TEM).

Thermogravimetric analysis (TGA) reveals some mass loss at about 100°C related to loss of adsorbed water (Fig. 5). The differential thermogravimetric (DTG) curve shows the temperature at which the maximum degradation weight loss occurs. At higher temperatures, the mass losses are related to phase changes, material degradation and loss of structural water. Above ~300°C cellulose nanofibrils rapidly lose mass due to their rapid degradation to CO_2 and H_2O, with stabilization (near total degradation with approximately 98% of mass loss) seen at ~530°C (Fig. 5a). For magnetite, a small mass loss occurs at around 200°C related to adsorbed water. After this, no mass loss is seen; however, an exothermic event is observed in the DTG curve (Fig. 5b) related to conversion of magnetite to maghemite. Magnetite can also convert directly to hematite but this conversion does not appear in DTG curve (Cornell & Schwertmann, 2003). The maghemite (γ-Fe_2O_3) and hematite (Fe_2O_3) are iron oxides such as magnetite, but

with different compositions and molecular arrangements. As expected, for the 1:1 cel:mag hybrids produced here (Fig. 5c), a 50% mass loss related to degradation of cellulose nanofibrils was confirmed with a change in DTG curve at around ~300°C corresponding to energy release. The other 50% of the mass is magnetite, which is not expected to degrade within this temperature range.

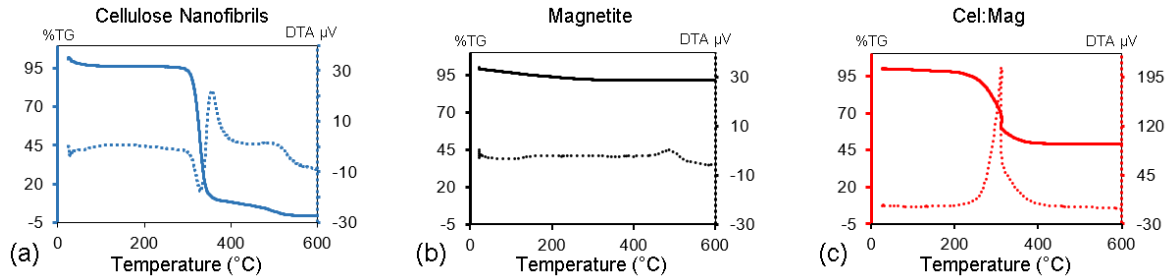

Fig. 5 Typical thermograms of thermogravimetric analysis (TGA) and differential thermogravimetric (DTG) curves of cellulose nanofibrils obtained with mechanical defibrillation (a); synthetized pure magnetite (b); and the hybrid catalyst (cel:mag) obtained with cellulose nanofibrils and magnetite (c).

Fig. 6a shows the FTIR spectra of the samples. For cellulose nanofibrils, bands are observed corresponding to OH groups at around 3600 and 3200 cm^{-1}; stretching of the CH bond at 2900 cm^{-1}; deformation of primary and secondary OH groups at 1640 cm^{-1} and 1400 cm^{-1} region; stretched CO group at 1100 cm^{-1} and bands related to alcohol groups below 1000 cm^{-1} (Silverstein & Webster, 1997). For magnetite, the characteristic bands are below 600 cm^{-1} and it is possible to identify a band at 590 cm^{-1} related to FeO interactions (Cornell & Schwertmann, 2003). For cel:mag, characteristic bands related to cellulose were seen, and the band of FeO that is interesting to catalysis, showing that Fe is available in the material.

Fig. 6b shows the X-ray diffractograms with some characteristic and well-defined peaks, at around 18° and 22° (Zugenmaier, 2008) corresponding to cellulose nanofibrils indicative of the presence of crystalline phases and agreeing with the findings of Vivekanandhan for microcrystalline cellulose. Well-defined peaks are observed for magnetite also indicating its crystalline character (shown with an enlarged scale since the intensity is much lower than that of pure cellulose) (Vivekanandhan, Christensen, Misra, & Mohanty, 2012) and confirming the efficiency of the synthesis. The magnetite diffractogram, according to the JCPDS data library (card number 88-315 for magnetite) refers to an iron oxide with a cubic crystalline phase

(Sasaki, 1997). For cel:mag, the diffractogram is practically identical to pure magnetite, with near perfect overlap, indicating that magnetite is well-dispersed within the matrix material.

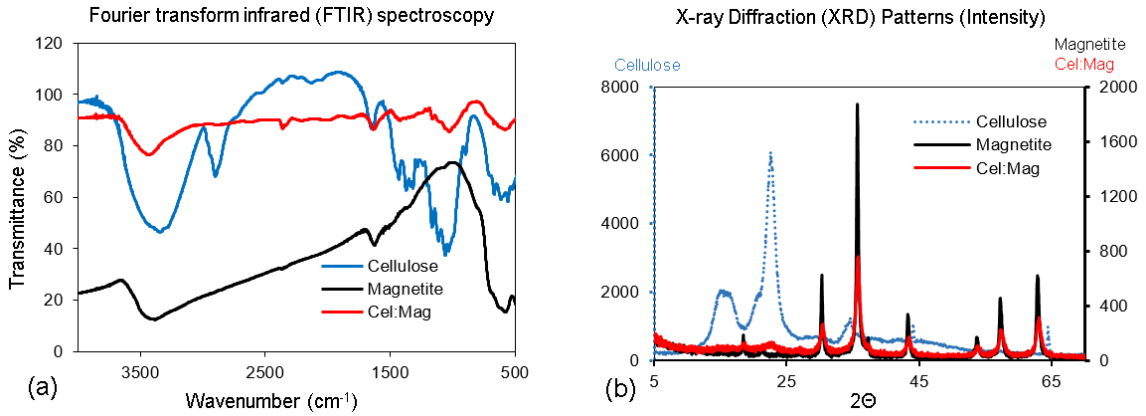

Fig. 6 (a). Typical Fourier transform infrared (FTIR) spectra of cellulose nanofibrils obtained with mechanical defibrillation (—Cellulose), synthetized pure magnetite (— Magnetite), and the hybrid catalyst obtained with cellulose nanofibrils and magnetite (—Cel:Mag) and (b). X-ray diffraction (XRD) patterns of cellulose nanofibrils obtained with mechanical defibrillation (.....Cellulose) using the scale on the left; and synthetized pure magnetite (— Magnetite) and the hybrid catalyst obtained with cellulose nanofibrils and magnetite (— Cel:Mag) using the scale on the right.

3.3. Catalytic properties

Catalytic potential of materials could be verified by performing a decomposition of H_2O_2 because this reaction, in consecutive steps, generates free radicals, highly reactive species that attack most organic molecules (Munoz, de Pedro, Casas, & Rodriguez, 2015). The reaction is monitored by measuring the formation of oxygen that is proportional to the decomposition of peroxide according the reaction $H_2O_2 \rightarrow H_2O + ½\ O_2$. The results for cel:mag and pure magnetite (Fig. 7) show that both materials decompose H_2O_2 which is evidenced by the increase in oxygen evolution over time. Magnetite generates a larger volume of oxygen than cel:mag under similar conditions perhaps due to the presence of twice the amount of Fe in pure magnetite compared to cel:mag. Cel:mag contains a 1:1 ratio of cellulose and magnetite.

Fenton-like process is a complex reaction and the exact mechanism is difficult to predict in heterogeneous systems. More details about the possible Fenton degradation mechanisms were reported elsewhere (He, Yang, Men, & Wang, 2016; Munoz, de Pedro, Casas, & Rodriguez, 2015). There are evidences that Fe^{2+} and Fe^{3+} catalyzes the generation of free hydroxyl radicals that degrade most of the organic compounds (He, Yang, Men, & Wang, 2016; Munoz, de Pedro, Casas, & Rodriguez, 2015; Nidheesh, Gandhimathi, & Ramesh, 2013; Rahim

Pouran, Abdul Raman, & Wan Daud, 2014). Therefore, in order to maintain catalytic activity and re-use the material for multiple cycles, Fe ions should be available on the surface of the catalyst and should not leach out with time. Leaching tests, using the supernatant of water and catalysts (cel:mag leached and magnetite leached), were performed to determine if Fe was lost from the catalyst to the reaction medium, resulting in a loss of catalytic activity. If Fe leaches, H_2O_2 is decomposed by a homogeneous catalysis using the supernatant of a catalyst solution. Fig. 7 shows the results of H_2O_2 decomposition using the leached materials and shows that no significant evolution of oxygen was observed, indicating that magnetite and cel:mag are not losing catalytic activity.

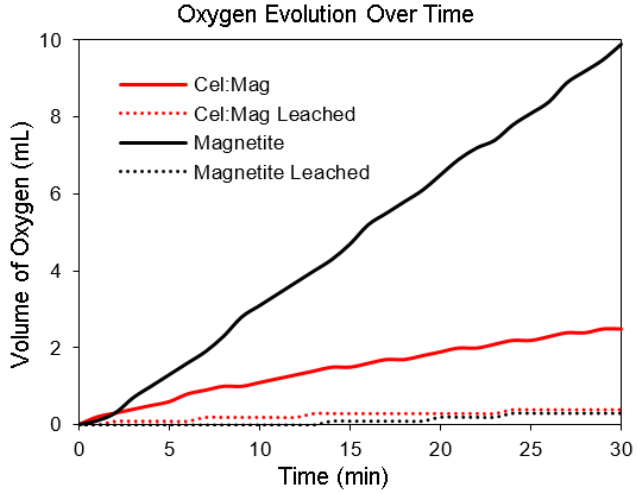

Fig. 7 Oxygen evolution over time in reactions of H_2O_2 decomposition using the hybrid catalyst obtained with cellulose nanofibrils and magnetite (— Cel:Mag), pure magnetite (— Magnetite), the leached hybrid catalyst (..... Cel:Mag Leached) and leached pure magnetite (..... Magnetite Leached) as catalysts.

The maintenance of catalytic activity was confirmed over 10 consecutive cycles of methylene blue decomposition (9.9 mL at 50 ppm, for 180 min) using the same catalyst sample with >95% discoloration for all 10 cycles (Fig. 8a). Catalytic potential of cel:mag and magnetite was evaluated by degradation kinetics using methylene blue as organic compound (Fig. 8b). The degradation was monitored by measuring the discoloration of the solution spectroscopically at 665 nm (Dhar, Kumar, & Katiyar, 2015). Methylene blue is a dye used as a model for de-activating a pollutant and the effectiveness of this degradation reaction indicates that the cel:mag catalyst could be used in treatment of effluents that generate large quantities of organic waste.

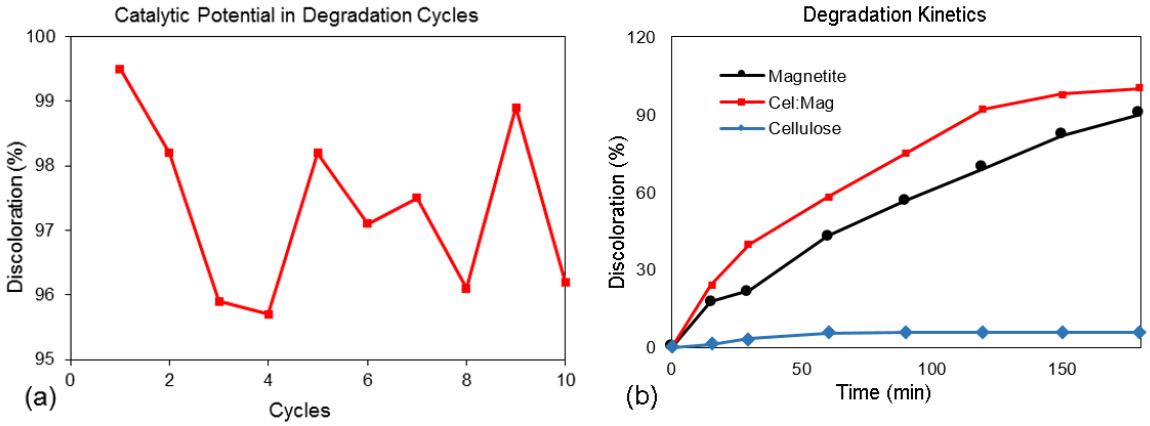

Fig. 8 Catalytic potential in consecutive cycles reusing the same amount of hybrid catalyst (cel:mag) obtained with cellulose nanofibrils and magnetite (a) and degradation kinetics using the hybrid catalyst (—Cel:Mag), pure magnetite (—Magnetite) and pure cellulose (— Cellulose) as catalysts (b) demonstrated in measures of discoloration (%) of methylene blue solution (50 ppm).

In 180 min, complete and 90% discoloration of methylene blue solution was observed following exposure to cel:mag and magnetite, respectively, indicating degradation of organic compound. Degradation kinetics is similar for both cel:mag and magnetite. However, cel:mag contains half the amount of magnetite as pure magnetite since half of the mass is cellulose; i.e., a 1:1 cel:mag has 5 mg of magnetite compared to 10 mg for pure magnetite. The positive results seen in Fig. 8b are likely due to the fact that Fe ions were more available in the cel:mag hybrid than in the magnetite, leading to similar reaction rates with the half amount of magnetite. The degradation kinetics performed with pure cellulose showed less than 6% discoloration (Fig. 8b), proving that Fe is necessary for catalysis and that discoloration of the solution is not due the absorption of dye by the cellulose.

4. Conclusions

A renewable hybrid catalyst was successfully produced from magnetite and cellulose nanofibrils. The material has potential to be used in Fenton-like reactions to degrade organic compound pollutants. Fe ions present in magnetite catalyzed the generation, from H_2O_2, of hydroxyl radicals that degraded methylene-blue dye, a compound presents in textile effluents. Cellulose nanofibrils were produced by mechanical defibrillation, resulting in a suspension of nanofibrils with an average diameter of 50 ±41 nm; 55% of the nanofibrils had diameters <40 nm. The synthesis of the hybrid catalyst, cel:mag, was verified performing SEM, TEM, surface

area, VSM, TGA, FTIR and XDR analysis and the results showed good dispersion of the magnetite on cellulosic surfaces. Leaching and re-use tests of the catalytic materials showed that they did not lose catalytic activity and can be used for multiple cycles. Degradation kinetics of H_2O_2 and methylene blue show complete (100%) and 90% discoloration within 180 min with the cel:mag hybrid and magnetite, respectively. Results showed that the magnetite (active phase), when dispersed in cellulosic matrix, degrades methylene blue dye, a model organic pollutant, at the same rate with less catalyst.

Acknowledgments

The authors thank: the National Council for Scientific and Technological Development (CNPq), Coordination for the Improvement of Higher Level Personnel (CAPES) and The Minas Gerais State Research Foundation (FAPEMIG) for financial support; Departments of Chemistry and Forestry Sciences at Federal University of Lavras for their outstanding infrastructure support; USDA, Bioproducts from Agricultural Feedstocks, Project Number: 2030-41000-058-00-D; Ron Weiss (Arkival Technology Corporation, Nashua, NH) for collecting the magnetometry measurements on the samples and for providing information for interpretation of the data; and Luiz Carlos A. Oliveira for surface area analysis.

References

Abe, K., & Yano, H. (2011). Formation of hydrogels from cellulose nanofibers. Carbohydrate Polymers, 85(4), 733-737.

Baetens, R., Jelle, B. P., & Gustavsen, A. (2011). Aerogel insulation for building applications: A state-of-the-art review. Energy and Buildings, 43(4), 761-769.

Bufalino, L., de Sena Neto, A. R., Tonoli, G. H. D., de Souza Fonseca, A., Costa, T. G., Marconcini, J. M., . . . Mendes, L. M. (2015). How the chemical nature of Brazilian hardwoods affects nanofibrillation of cellulose fibers and film optical quality. Cellulose, 22(6), 3657-3672.

Chen, W., Abe, K., Uetani, K., Yu, H., Liu, Y., & Yano, H. (2014). Individual cotton cellulose nanofibers: Pretreatment and fibrillation technique. Cellulose, 21(3), 1517-1528.

Chin, S. F., Binti Romainor, A. N., & Pang, S. C. (2014). Fabrication of hydrophobic and magnetic cellulose aerogel with high oil absorption capacity. Materials Letters, 115, 241-243.

Cornell, R. M., & Schwertmann, U. (2003). Introduction to the Iron Oxides. In R. M. Cornell & U. Schwertmann (Eds.), The Iron Oxides: Structure, Properties, Reactions, Occurences and Uses, Second Edition (pp. 1-7). Weinheim, FRG.: Wiley-VCH Verlag GmbH & Co. KGaA

Dhar, P., Kumar, A., & Katiyar, V. (2015). Fabrication of cellulose nanocrystal supported stable Fe(0) nanoparticles: a sustainable catalyst for dye reduction, organic conversion and chemo-magnetic propulsion. Cellulose, 22(6), 3755-3771.

Eichhorn, S. J., Dufresne, A., Aranguren, M., Marcovich, N. E., Capadona, J. R., Rowan, S. J., . . . Peijs, T. (2010). Review: Current international research into cellulose nanofibres and nanocomposites. Journal of Materials Science, 45(1), 1-33.

Fengel, D., & Wegener, G. (1984). Wood: chemistry, ultrastructure, reactions. Berlin: Walter de Gruyter.

Fonseca, C. S., da Silva, T. F., Silva, M. F., Oliveira, I. R. C., Mendes, R. F., Hein, P. R. G., . . . Tonoli, G. H. D. (2016). Eucalyptus cellulose micro/nanofibrils in extruded fibercement composites. Cerne, 22(1), 59-68.

Gericke, M., Trygg, J., & Fardim, P. (2013). Functional cellulose beads: Preparation, characterization, and applications. Chemical Reviews, 113(7), 4812-4836.

Heath, L., & Thielemans, W. (2010). Cellulose nanowhisker aerogels. Green Chemistry, 12(8), 1448-1453.

He, J., Yang, X., Men, B., & Wang, D. (2016). Interfacial mechanisms of heterogeneous Fenton reactions catalyzed by iron-based materials: A review. Journal of Environmental Sciences, 39, 97–109.

Innerlohinger, J., Weber, H. K., & Kraft, G. (2006). Aerocellulose: Aerogels and aerogel-like materials made from cellulose. Macromolecular Symposia, 244, 126-135.

Liu, S., Yan, Q., Tao, D., Yu, T., & Liu, X. (2012). Highly flexible magnetic composite aerogels prepared by using cellulose nanofibril networks as templates. Carbohydrate Polymers, 89(2), 551-557.

Luo, X., & Zhang, L. (2009). High effective adsorption of organic dyes on magnetic cellulose beads entrapping activated carbon. Journal of Hazardous Materials, 171(1-3), 340-347.

Munoz, M., de Pedro, Z. M., Casas, J. A., & Rodriguez, J. J. (2015). Preparation of magnetite-based catalysts and their application in heterogeneous Fenton oxidation - A review. Applied Catalysis B: Environmental, 176-177, 249-265.

Nakagaito, A. N., & Yano, H. (2004). The effect of morphological changes from pulp fiber towards nano-scale fibrillated cellulose on the mechanical properties of high-strength plant fiber based composites. Applied Physics A: Materials Science and Processing, 78(4), 547-552.

Nidheesh, P. V., Gandhimathi, R., & Ramesh, S. T. (2013). Degradation of dyes from aqueous solution by Fenton processes: A review. Environmental Science and Pollution Research, 20(4), 2099–2132.

Nogueira, R. F., Trovó, A. G., Da Silva, M. R. A., Villa, R. D., & De Oliveira, M. C. (2007). Fundaments and environmental applications of Fenton and photo-Fenton processes. Quimica Nova, 30(2), 400-408.

Oksman, K., Aitomäki, Y., Mathew, A. P., Siqueira, G., Zhou, Q., Butylina, S., . . . Hooshmand, S. (2016). Review of the recent developments in cellulose nanocomposite processing. Composites Part A: Applied Science and Manufacturing, 83, 2-18.

Olsson, R. T., Azizi Samir, M. A. S., Salazar Alvarez, G., BelovaL, StromV, Berglund, L. A., . . . Gedde, U. W. (2010). Making flexible magnetic aerogels and stiff magnetic nanopaper using cellulose nanofibrils as templates. Nature Nanotechnology, 5(8), 584-588.

Rahim Pouran, S., Abdul Raman, A. A., & Wan Daud, W. M. A. (2014). Review on the application of modified iron oxides as heterogeneous catalysts in Fenton reactions. Journal of Cleaner Production, 64, 24–35.

Reza, M. T., Rottler, E., Tölle, R., Werner, M., Ramm, P., & Mumme, J. (2015). Production, characterization, and biogas application of magnetic hydrochar from cellulose. Bioresource Technology, 186, 34-43.

Sasaki, S. (1997). Radial Distribution of Electron Density in Magnetite, Fe3O4. Acta Crystallographica Section B: Structural Science, 53(5), 762-766.

Schwertmann, U., & Cornell, R. M. (2000). Iron Oxides in the Laboratory: Preparation and Characterization, Second edition. Weinheim: Wiley-VCH Verlag GmBH.

Silverstein, R. M., & Webster, F. X. (1997). Spectrometric Identification of Organic Compounds, 6th edition. London: John Wiley & Sons.

Small, A. C., & Johnston, J. H. (2009). Novel hybrid materials of magnetic nanoparticles and cellulose fibers. Journal of Colloid and Interface Science, 331(1), 122-126.

Tonoli, G. H. D., Fuente, E., Monte, C., Savastano Jr, H., Lahr, F. A. R., & Blanco, A. (2009). Effect of fibre morphology on flocculation of fibre-cement suspensions. Cement and Concrete Research, 39(11), 1017-1022.

Tonoli, G. H. D., Holtman, K. M., Glenn, G., Fonseca, A. S., Wood, D., Williams, T., . . . Orts, W. J. (2016). Properties of cellulose micro/nanofibers obtained from eucalyptus pulp fiber treated with anaerobic digestate and high shear mixing. Cellulose, 23, 1239-1256.

Tonoli, G. H. D., Rodrigues Filho, U. P., Savastano Jr, H., Bras, J., Belgacem, M. N., & Rocco Lahr, F. A. (2009). Cellulose modified fibres in cement based composites. Composites Part A: Applied Science and Manufacturing, 40(12), 2046-2053.

Uetani, K., & Yano, H. (2011). Nanofibrillation of wood pulp using a high-speed blender. Biomacromolecules, 12(2), 348-353.

Vivekanandhan, S., Christensen, L., Misra, M., & Mohanty, A. K. (2012). Green Process for Impregnation of Silver Nanoparticles into Microcrystalline Cellulose and Their Antimicrobial Bionanocomposite Films. Journal of Biomaterials and Nanobiotechnology, 3, 371-376.

Wan, C., & Li, J. (2015). Synthesis of well-dispersed magnetic CoFe2O4 nanoparticles in cellulose aerogels via a facile oxidative co-precipitation method. Carbohydrate Polymers, 134, 144-150.

Wang, H., Li, D., Yano, H., & Abe, K. (2014). Preparation of tough cellulose II nanofibers with high thermal stability from wood. Cellulose, 21(3), 1505-1515.

Zhu, W., Ma, W., Li, C., Pan, J., & Dai, X. (2015). Well-designed multihollow magnetic imprinted microspheres based on cellulose nanocrystals (CNCs) stabilized Pickering double emulsion polymerization for selective adsorption of bifenthrin. Chemical Engineering Journal, 276, 249-260.

Zugenmaier, P. (2008). Crystalline Cellulose and Derivatives, 1st edition. Berlin: Springer.

ARTIGO 2

Bio-based thin films for application in green electronics

"Versão Preliminar"

Ana Carolina Cunha Arantes[1], Luiz Eduardo Silva[2], Delilah F. Wood[3], Crislaine das Graças Almeida[1], Gustavo Henrique Denzin Tonoli[2], Juliano Elvis de Oliveira[4], Joaquim Paulo da Silva[5], Willian J. Orts[3], Maria Lucia Bianchi[1]

[1] Department of Chemistry, Federal University of Lavras, CP 3037, Lavras- MG, Brazil.
[2] Department of Forest Sciences, Federal University of Lavras, CP 3037, Lavras- MG, Brazil.
[3] Bioproducts Research Unit, WRRC, ARS- USDA, Albany, CA 94710, USA.
[4] Department of Engineering, Federal University of Lavras, CP 3037, Lavras- MG, Brazil.
[5] Department of Physics, Federal University of Lavras, CP 3037, Lavras- MG, Brazil.

Abstract

In this study, bio-based thin films were developed for use in the production of green electronics in order to reduce the generation of toxic and nonrenewable e-waste. The films composed of cellulose nanofibrils, chitosan, magnetite and glycerol were prepared by a solution casting and characterized chemically and physically using Fourier transform infrared spectroscopy, thermal, mechanical and water vapor transmission analysis, surface free energy, wettability and electrical measurements. Results showed the influence of magnetite and the plasticizer, glycerol, on films properties. Measures of capacitance and calculation of dielectric constant show a potential to use the films as dielectric in capacitors.

Keywords: cellulose nanofibrils; biopolymers; plasticizer; dielectric constant; capacitor.

Introduction

The electronic industry has grown exponentially over the past 50 years, due to the advancement of telecommunications and information technology (Tansel, 2017; Zeng, Yang, Chiang, & Li, 2017). Consequently, the generation of electrical and electronic waste, the "e-waste", become a global concern in terms of environmental impacts. In 2015, the e-waste production was around 43 million tons and is estimated that in 2018, this number will be around 50 million tons (Kumar & Holuszko, 2016; Tansel, 2017). These wastes contain a large amount of toxic materials and are not biodegradable (Zeng et al., 2017). There are many studies about new technologies to treatment of e-waste (Kumar & Holuszko, 2016; Nowakowski, 2016; Zeng et al., 2017), but an alternative to reduce the environmental impact is develop the green electronics using renewable and non-toxic materials, like bio-based hybrid materials, in production of electronic devices (S. Liu, Yu, Wu, Li, & Li, 2014; Tansel, 2017).

There are many areas involved in electronic industry, like data storage, information management and device development, and all this areas requires batteries and storage of charge (Share, Westover, Li, & Pint, 2016). Capacitors are devices present in various electronics used to store electric charge (Kötz & Carlen, 2000). They have a pair of conductor plates separated by a dielectric that is used to avoid the contact between the conductor plates of the capacitor and increases the capacity to store charge, comparing to vacuum, in a factor named dielectric constant (εr) (Li et al., 2016; Nishino, 1996; Rana, Johri, & Asokan, 2013).

New materials have been studied to be used as dielectric in order to reduce the generation of e-waste. Renewable and non-toxic hybrid materials composed by biopolymers (cellulose and chitosan) and iron oxides (magnetite) are presented as an alternative (Ali-zade, 2015; S. Liu et al., 2014; Vellakkat & Hundekal, 2017). From the hybrids can be produced thin films using a plasticizer agent (glycerol), to be used like a dielectric in capacitors (Ayala, Agudelo, Paz, & Vargas, 2011; da Silva et al., 2017; Morgado et al., 2013).

Cellulose and chitosan are the two most abundant biopolymers on earth. They are renewable, biocompatible and biodegradable. They have a good interaction between them because of the similarity of chemical structure (Abdul Khalil et al., 2016; Thakur & Voicu, 2016). Both are insoluble in water, but from cellulose can be produced cellulose nanofibrils that form a stable suspension on water due to the nanometric scale and chitosan can be diluted in weak acids. Cellulose and chitosan can be used as matrix to produced hybrid nanofilms (Hassan, Hassan, Abou-zeid, & El-Wakil, 2016). To use the films in electrical applications, can be add

magnetite in the hybrid, an iron oxide magnetic and easy to obtain, that confers good parameters to the films (Cornell & Schwertmann, 2003; Su, 2017). The films could be plasticized using glycerol, that is renewable and biodegradable, to obtain a flexible films (Y. Liu, Sun, Wang, & Ni, 2016).

In this context, the aim of this study was to evaluate the impact of using magnetite and glycerol (plasticizer) on physical-chemical properties of cellulose/chitosan based films and verify the dielectric constant of the films to be used in capacitors.

Materials and methods

Materials

Cellulose nanofibrils were obtained from fibers of commercial eucalyptus kraft pulp (Jacareí/SP, Brazil) by mechanical defibrillation of the fiber cell wall using a SuperMasscolloider, Masuko Sangyo MKCA6-3 (Japan), operated at 1500 rpm, with a 0.01 mm opening between disks. The fibers were immersed in distilled water for 48 h at 1% (w/w) concentration and applying 35 passages through the defibrillator to obtain a suspension of nanofibrils (Arantes et al., 2017; Bufalino et al., 2015; Tonoli et al., 2016). Chitosan solution (Polymar Industry, Fortaleza/CE, Brazil) were prepared mixing 2% in mass of chitosan with a solution of acetic acid (IMPEX) 0,5%. Magnetite were synthetized on suspension of cellulose nanofibrils (Arantes et al., 2017) where Fe^{2+} and Fe^{3+} salts (6.314 g of FeCl3 and 2.343 g of $FeCl_2$) were dissolved in 200 mL of an aqueous suspension of cellulose nanofibrils under nitrogen flow. NH_4OH was added until pH 11 and was attained to precipitate both magnetite and cellulose from solution. The precipitate was washed with water until approximately pH 7 and solubilized in 100 mL of distilled water. The plasticizer agent was glycerol (VETEC) 99,5%.

Films production

The components were mixed for 30 min and the films were prepared by a solution casting on acrylic plates at 50°C for 24 h. The CEL:CHI:GLY film contain 100 mL of cellulose nanofibrils suspension, 100 mL of chitosan solution and 1 mL of glycerol; CEL:CHI:MAG:GLY film contain 100 mL of magnetite and cellulose nanofibrils solution, 100 mL of chitosan and 1 mL of glycerol; and CEL:CHI:MAG film contain 100 mL of magnetite and cellulose nanofibrils solution and 100 mL of chitosan solution.

Infrared analysis

Fourier transform infrared spectroscopy (FTIR) was performed using a Varian 660 spectrophotometer coupled with GladiATR (Pike Technologies), with a monolithic diamond, in the spectral range of 400 to 4400 cm^{-1}, at a 4 cm^{-1} resolution with 16 scans.

Thermal analysis

Thermal analysis was performed using a Shimadzu DTG-60AH TGA (Shimadzu Corporation, Kyoto, Japan). Samples of approximately 7 mg were heated under nitrogen atmosphere in the range of 40 to 650°C with a heating rate of 10°C.min^{-1} and a gas flow rate of 50 mL.min^{-1}.

Mechanical analysis

Mechanical tests were performed according to D882-02 (ASTM, 2002) standard in a TA.XTPlus Stable Micro Systems texture analyzer (England) with a 1 kN load cell. Five samples were cut into 70 x 10 mm strips and the initial separation between the grips was 20 mm, with a crosshead speed of 1.8 mm/min. The mechanical tests were done at 23°C. Tensile strength (TS) was calculated by dividing the maximum force by the initial cross-section area of the films. The percentage of elongation (E) was calculated by dividing the strain at specimens rupture by the initial gauge length and multiplying by 100. Modulus of elasticity (ME) was calculated from the slope in the range of linear proportionality of the stress-strain curves, whose stress (expressed in Pa) is the force (measured in N) per unit area and strain (mm/mm) is the change in length per unit length (measured in mm).

Water vapor transmission analysis

The water vapor transmission measurements were performed according to the E96/ E96M (ASTM, 2016) standard. Five samples of each film were put in permeation cells containing silica and conditioned in desiccators with relative humidity of 100%, at around 23°C. The measures of changes on weight of the films were made per 96 hours. The water vapor transmission rate (WVTR) was calculated using Eq.1:

$$WVTR = \frac{w}{t*A} \qquad [1]$$

where w is the mass (g) of the permeation cell, t is time (h) and A is the exposed area of the film (m²). The water vapor permeability (WVP) was calculated using Eq.2:

$$WVP = \frac{(WVTR * T * 100)}{(P_{H_2O} * \Delta H)} \quad [2]$$

where T is thickness of the films (m), p_{H2O} is the water vapor pressure and ΔH is the difference between humidity inside and outside of the permeation cell. The film thickness was measured in 5 different points in a 3 cm^2 area using an electronic micrometer Digimess (± 0.001 mm).

Surface free energy and wettability

Contact angle measurements were performed depositing calibrated droplets of liquids with different polarities (Table 1) on the films. Wettability was verified based on contact angle of water droplets and surface energy of the films were determined according to Tonoli, et al. (2009) calculating the dispersive and polar components. The apparatus used was a drop shape analyzer Krüss DSA25, equipped with a CCD camera working at up to 200 images per second.

Table 1. Contact angle measurement probes and their characteristics.

Probe	Surface tension (mJ/m²)		
	Dispersive	Polar	Total
Water	21.8	51.0	72.8
Glycerol	21.2	41.5	62.7
Toluene	26.1	2.3	28.4
n-Hexane	18.4	0.0	18.4

Electrical measurements

The electrical properties of the films were verified with a parallel plate analysis in a LCR Meter Agilent U1733C (CA, United States) using insulated plates to hold the films (Fig. 1).

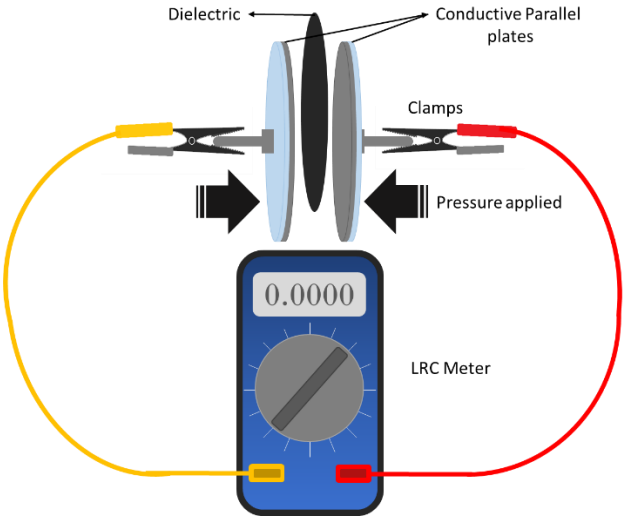

Fig. 1 Apparatus for electrical measurements.

Measurements of capacitance (expressed in Farad) were taken in two different frequencies (100 Hz and 1000 Hz) at 23°C. The dielectric constant (ε_r) were calculated from capacitance according to Eq 3:

$$\varepsilon_r = \frac{(C*t)}{(\varepsilon_0*A)} \qquad [3]$$

where C is the maximum capacitance at a determinate frequency (F), t is the thickness of the film (m), ε_0 is the dielectric constant of vacuum (8,85 x 10^{-12} F·m^{-1}) and A is the area (m^2) of the plates that hold the film.

Results and discussion

Bio-based hybrid thin films

The prepared films were named according to their composition, wherein CEL is cellulose nanofibrils, CHI is chitosan solution, MAG is magnetite and GLY is glycerol. The films presented homogeneous aspect, with suitable dispersion of the constituents. Film without magnetite present light coloration (Fig. 2A) and no magnetic properties (Fig. 2G) while films with magnetite present dark coloration (Fig. 2B and 2C) and magnetic characteristics (Fig. 2H

and 2I). Films with glycerol present high malleability (Fig. 2D and 2E), while films with no glycerol are stiffer and breakable (Fig. 2F).

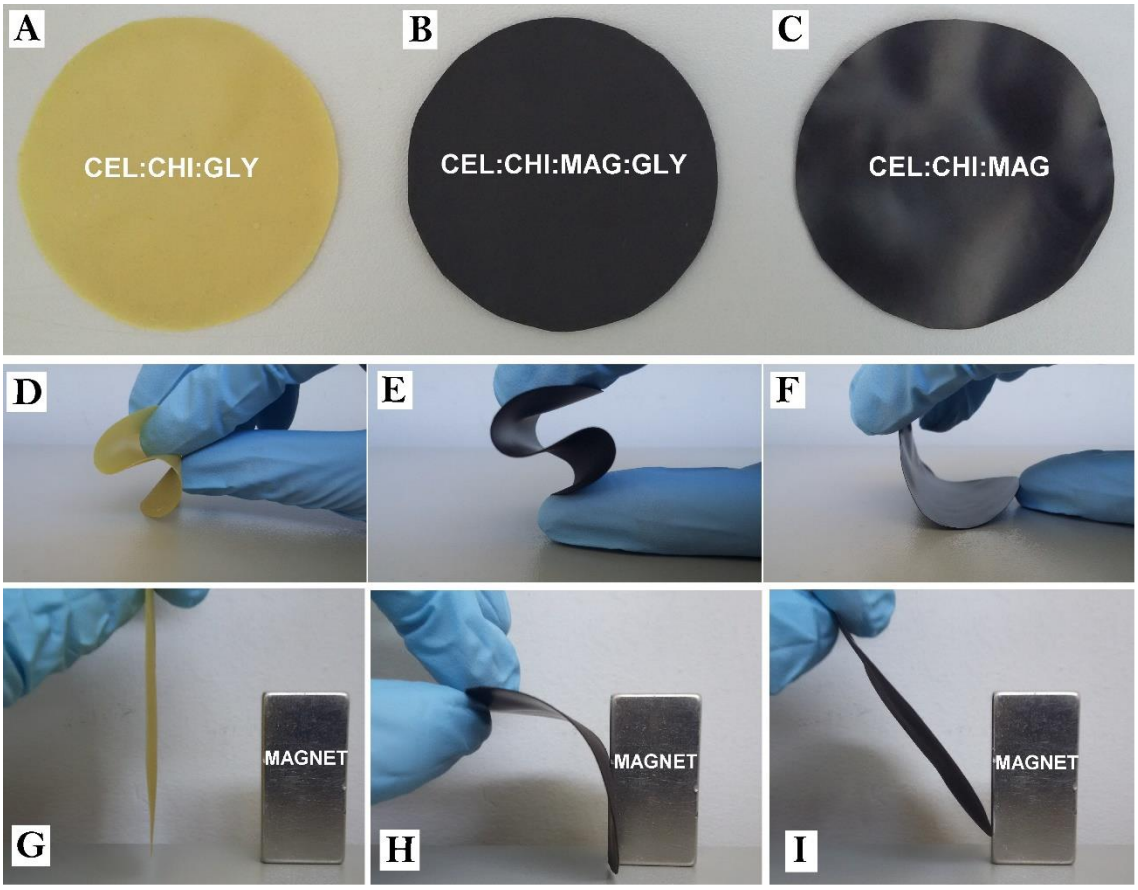

Fig. 2 From top to bottom: visual aspect, malleability and magnet property, demonstrated when the film is attracted by a magnet, of the films containing A, D and G) cellulose nanofibrils, chitosan and glycerol (CEL:CHI:GLY), B, E and H) cellulose nanofibrils, chitosan, magnetite and glycerol (CEL:CHI:MAG:GLY) and C, F and I) cellulose nanofibrils, chitosan and magnetite (CEL:CHI:MAG).

Physicochemical properties of the films

FTIR analysis was performed in order to determine the chemical changes after blending of the constituents and Fig. 3 depicts the FTIR spectra of the film samples. The band at around 3500 and 3100 cm^{-1} corresponds to OH bond stretching of the cellulose nanofibrils, chitosan and glycerol, and overlaps the NH bond stretching of chitosan. The peaks at 2930 cm^{-1} and 2870 cm^{-1} correspond to symmetric and asymmetric CH vibrations. All spectra present a peak at around 1630 cm^{-1} corresponding of CO stretching and NH bending of amide groups of chitosan, and deformation of primary and secondary OH groups. A peak at around 1560 cm^{-1} corresponding to vibration of protonated amino groups of chitosan. The bands at 1110 cm^{-1} and

below 1000 cm^{-1} are related to alcohol groups (Celebi & Kurt, 2015; Dias et al., 2014; Kongjao, Damronglerd, & Hunsom, 2010; Silverstein & Webster, 1997; Zhu, Bao, Wei, Ma, & Kong, 2016). For magnetite, the characteristic band is below 600 cm^{-1} related to FeO interactions, which is difficult to identify from this spectra (Cornell & Schwertmann, 2003).

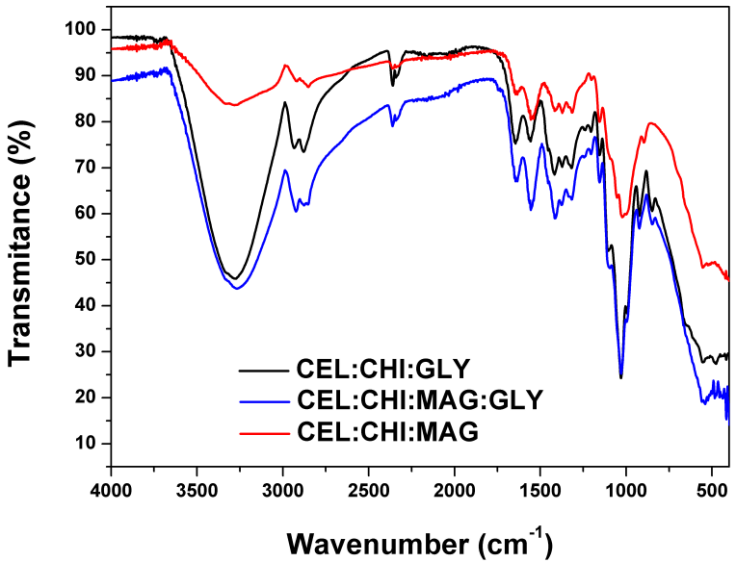

Fig. 3 Typical Fourier transform infrared (FTIR) spectra of films containing cellulose nanofibrils, chitosan and glycerol (CEL:CHI:GLY), cellulose nanofibrils, chitosan and magnetite (CEL:CHI:MAG) and cellulose nanofibrils, chitosan, magnetite and glycerol (CEL:CHI: MAG:GLY).

The TGA curves analysis showed mass loss (5%) for all groups around 25-100° C, resulted from water/moisture loss, with an endothermic event (DTA) in all thermograms (Fig. 4). The CEL:CHI:GLY and CEL:CHI:MAG:GLY films present mass loss at around 150 to 230°C with an endothermic event due to the decomposition of glycerol (Castelló, Dweck, & Aranda, 2009). The films present a rapidly loss of mass in the range of 230 to 350°C that refers to decomposition of cellulose nanofibrils and chitosan (Arantes et al., 2017; Hong et al., 2007; Leal, Ramos, Barrett, Curvelo, & Rodella, 2015). Between 350 and 650°C occurs the mass loss related to residual components of the films. There was around 20% of residual mass at 700°C for films with magnetite, because it is converted to other iron oxides such as maghemite or hematite (Schwertmann & Cornell, 2000), while there was just 5% of residues for films without magnetite.

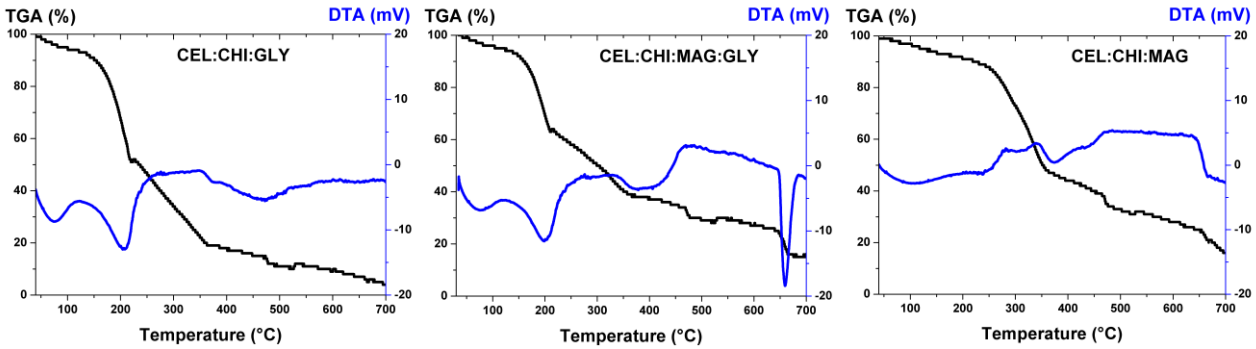

Fig. 4 Typical thermogravimetric (TGA) and differential thermal analysis (DTA) curves of films containing cellulose nanofibrils, chitosan and glycerol (CEL:CHI:GLY), cellulose nanofibrils, chitosan, magnetite and glycerol (CEL:CHI:MAG:GLY) and cellulose nanofibrils, chitosan and magnetite (CEL:CHI:MAG).

The tensile tests were performed to predict the behavior of the films when submit to an external force that can be applied at process to build devices using the films as component. Tensile strength (TS) measure the force or stress required to breaks a sample and is relate to the hardness of products. TS of the CEL:CHI:MAG films are higher than CEL:CHI:GLY and CEL:CHI:MAG:GLY. Glycerol is a plasticizing agent that improves the flexibility (Fig. 5) of biopolymer films, and it led to much lower TS values. The chemical bonds in the CEL:CHI:MAG films are stronger and lead to a stiffer structure to the film. This is also clearly verified by the lower percentage of elongation (E) of the films without glycerol, while the films containing glycerol present the highest E values (Table 2).

Table 2. Average and standard deviation values of tensile strength (TS), percentage of elongation (E), and modulus of elasticity (ME) of films containing cellulose nanofibrils, chitosan and glycerol (CEL:CHI:GLY), cellulose nanofibrils, chitosan, magnetite and glycerol (CEL:CHI:MAG:GLY) and cellulose nanofibrils, chitosan and magnetite (CEL:CHI:MAG).

	CEL:CHI:GLY	**CEL:CHI: MAG:GLY**	**CEL:CHI:MAG**
TS (MPa)	9.8 ± 0.8	8.8 ± 0.4	44.0 ± 1.7
E (%)	37.0 ± 3.4	33.0 ± 0.7	8.3 ± 0.5
ME (MPa)	30.0 ± 1.1	25.0 ± 1.3	1545.0 ± 20.0

The modulus of elasticity (ME) is a measure of rigidity of a sample. Values of ME (Table 2) are consistent with the discussion about TS, where films without glycerol (CEL:CHI:MAG) present much higher values of ME than films with glycerol. Glycerol has a low molecular weight and can occupy intermolecular spaces between biopolymer chains,

reducing secondary forces among them. Also, glycerol change the three-dimensional molecular organization of chitosan, reducing the energy required for molecular mobility and the formation of hydrogen bonding between the chains. As a consequence, an increase in the free volume and, hence, an increase in biopolymer film flexibility, and decreases in hardness are observed (Sanyang, Sapuan, Jawaid, Ishak, & Sahari, 2015).

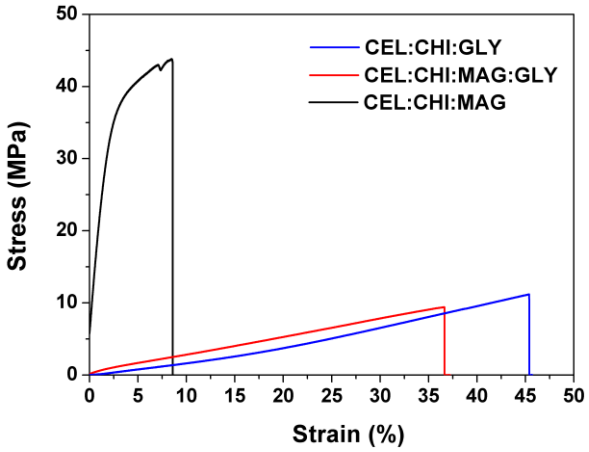

Fig. 5 Stress *vs* strain curves of films containing cellulose nanofibrils, chitosan and glycerol (CEL:CHI:GLY), cellulose nanofibrils, chitosan, magnetite and glycerol (CEL:CHI: MAG:GLY) and cellulose nanofibrils, chitosan and magnetite (CEL:CHI:MAG).

Water vapor transmission analysis provides the barrier property of the films because verify how the water vapor flows through the surface. The composition of the films can be modified to increase or block the passage of vapor (ASTM, 2016; Costa et al., 2016; Seoane, Fortunati, Puglia, Cyras, & Manfredi, 2016). The values of water vapor transmission rate (WVTR) and water vapor permeability (WVP) of the films are presented on Table 3. Addition of plasticizers (glycerol) improved water vapor barrier properties of chitosan/ cellulose based films. This increase can be attributed to the high affinity of glycerol to water. Glycerol is a relatively small hydrophilic molecule and may be easily inserted between chitosan and cellulose macromolecules to establish hydrogen bonds with hydroxyl groups of cellulose and amine in chitosan (Lamim et al., 2006; Yoshida, Oliveira, & Franco, 2009). The presence of glycerol on films increase the water absorption due to highly hydrophilic characteristic, comparing WVP values to the films with glycerol (CEL:CHI:GLY and CEL:CHI:MAG:GLY) and the films without glycerol (CEL:CHI:MAG). Besides that, glycerol modifies the film structure increasing the free volume on matrix (Y. Liu et al., 2016), increasing the rate that water vapor flows through the film surface, that is WVTR values.

Table 3. Water vapor permeability (WVP) and water vapor transmission rate (WVTR) of films containing cellulose nanofibrils, chitosan and glycerol (CEL:CHI:GLY), cellulose nanofibrils, chitosan, magnetite and glycerol (CEL:CHI:MAG:GLY) and cellulose nanofibrils, chitosan and magnetite (CEL:CHI:MAG).

	CEL:CHI:GLY	CEL:CHI: MAG:GLY	CEL:CHI:MAG
WVP	2.8 ± 0.1	3.6 ± 0.2	1.6 ± 0.1
WVTR	40.0 ± 1.2	41.4 ± 1.9	34.0 ± 0.4

In addition to water vapor transmission tests, it was performed a wettability analysis. The wettability is the ability of a liquid to maintain contact with a solid and it is determined by the measurement of the contact angle formed between a liquid drop and the material surface (Yuan & Lee, 2013). The angles formed between the water drop and the films surfaces (Fig. 6) show the higher hydrophilic character of the films with glycerol. Contact angles higher than 90° represent less hydrophilic surfaces or low wettability, while angles lower than 90° represent more hydrophilic surface or high wettability (Han, Sun, Zheng, Li, & Jin, 2016; Luz, Ribeiro, & Pandolfelli, 2008; Yuan & Lee, 2013). Films prepared with glycerol present lower contact angles with water because glycerol is hygroscopic and influence on wettability of the films. It seems that magnetite led to increased contact angle, hence the interaction of the water drop with hydroxyl groups of cellulose and amine groups of chitosan are lower, and resulting on less available bonds with water.

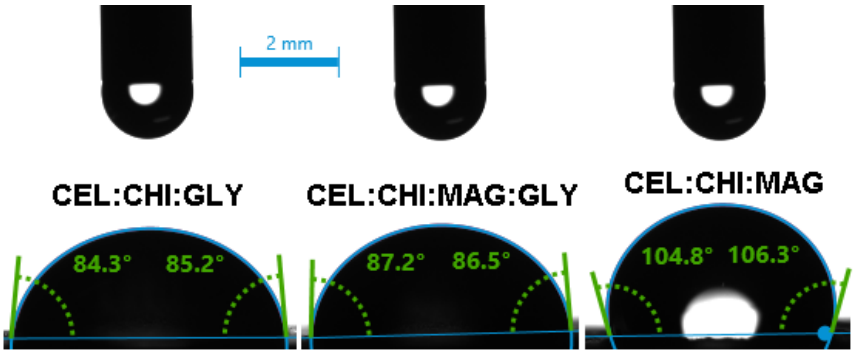

Fig. 6 Contact angle of water drops on films containing cellulose nanofibrils, chitosan and glycerol (CEL:CHI:GLY), cellulose nanofibrils, chitosan, magnetite and glycerol (CEL:CHI:MAG:GLY) and cellulose nanofibrils, chitosan and magnetite (CEL:CHI:MAG).

The surface free energy (SFE) is a parameter that presents the excess of energy in the surface of a solid and can be correlated with the adhesion of a material to another component

(Owens & Wendt, 1969). The SFE is measured based on contact angles of a surface with different solvents. Fig. 7 presents the polar and dispersive contributions to the surface energy of the films. The SFE is nearly the same to the films, showing a similar dispersive contribution, but a slightly decrease on polar contribution when adding magnetite, comparing CEL:CHI:GLY and CEL:CHI:MAG:GLY, and removing glycerol, comparing CEL:CHI:MAG:GLY and CEL:CHI:MAG (Fig. 7) (Shahbazi, Rajabzadeh, Rafe, Ettelaie, & Ahmadi, 2016). The effect of glycerol on polar component is due to the hydrophilicity, same as in wettability. The amount of hydroxyl groups increases with addition of glycerol leading to a higher interaction with water, resulting an increase on polar component.

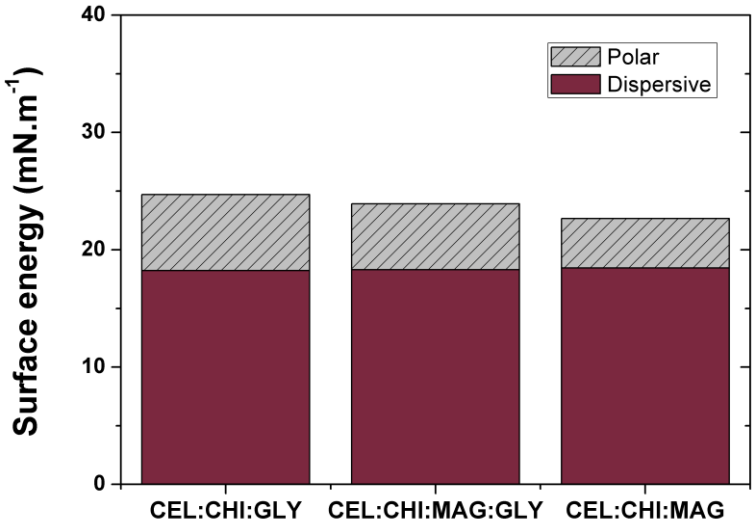

Fig. 7 Surface energy components (polar and dispersive) of films containing cellulose nanofibrils, chitosan and glycerol (CEL:CHI:GLY), cellulose nanofibrils, chitosan, magnetite and glycerol (CEL:CHI:MAG:GLY) and cellulose nanofibrils, chitosan and magnetite (CEL:CHI:MAG).

Electrical applications

The capacitance of the films, expressed in Farad (F), measured in two different frequencies (100 and 1000 Hz) and the calculated dielectric constant (ε_r) are presented in Fig. 8. The measures were taken in two frequencies to verify the behavior of a dielectric material, wherein it is expected that for higher frequencies the dielectric presents lower capacitance, a phenomenon known as dielectric dispersion (Bhatt, Krishna Bhat, & Santosh, 2010; Boukheir et al., 2017). At 1000 Hz, the capacitance of the films are lower than at 100 Hz, leading to a lower permittivity of the dielectric. The increase of frequency leads to a decrease of

polarization, due to a delay in changes of charges, reaching a constant value in a certain frequency.

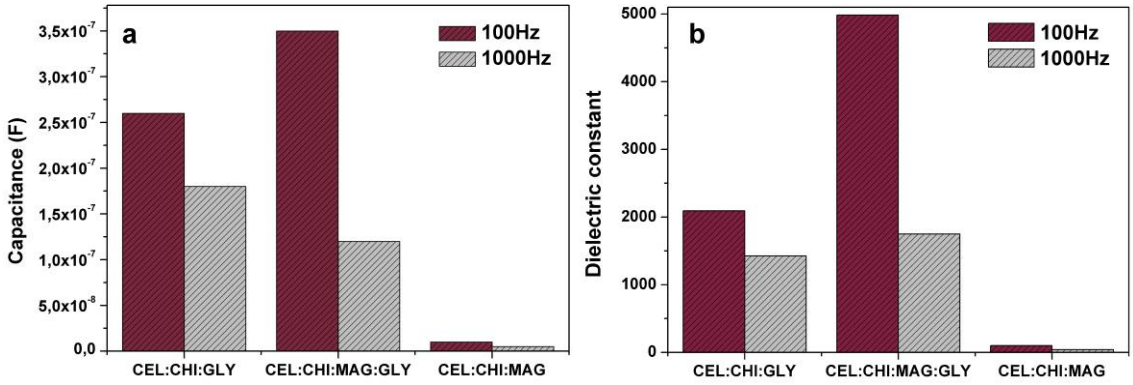

Fig. 8 a) Capacitance and b) dielectric constant graphs of the films containing cellulose nanofibrils, chitosan and glycerol (CEL:CHI:GLY), cellulose nanofibrils, chitosan, magnetite and glycerol (CEL:CHI:MAG:GLY) and cellulose nanofibrils, chitosan and magnetite (CEL:CHI:MAG).

The dielectric constant is an important property for using the films as dielectric in capacitors. Films without glycerol (CEL:CHI:MAG) presents small ε_r compared to films with glycerol, although the CEL:CHI:MAG films present values (ε_r=10) higher than paper(ε_r=3). The ε_r of the films produced with glycerol increased probably because the glycerol fill the gaps between the components of the films, facilitating the permittivity of the material. At 100 Hz, CEL:CHI:GLY presents ε_r values of around 2100 and CEL:CHI:MAG:GLY presents ε_r values of around 4900. Besides the contribution of glycerol, the magnetite has influence on permittivity, because it is a magnetic compound (Bhatt et al., 2010; Pang, Khoh, & Chin, 2011). The electric field can be associated with magnets because the magnetic flux results in an electric field know as electromagnetic field (Ali-zade, 2015). In addition, magnetite can form a connectivity through the film and reach the percolation threshold improving the charge movement. The contribution of magnetite and the ε_r value makes the CEL:CHI:MAG:GLY film with great potential to be used as a dielectric in a capacitors.

Conclusions

Bio-based thin films were successfully produced from cellulose nanofibrils (CEL), chitosan (CHI), magnetite (MAG) and glycerol (GLY) and they have potential to be used as dielectric in capacitors. The films, CEL:CHI:GLY, CEL:CHI:MAG:GLY and CEL:CHI:MAG

was produced by casting and present an homogeneous aspect and good dispersion between the components. Physical-chemical characteristics of the films was verified performing FTIR, thermal, mechanical and water vapor transmission analysis, surface free energy and wettability and the results showed the influence of the plasticizer on properties of the films. Glycerol provides flexibility, a higher wettability and lower barrier property. The dielectric constant calculations presents the influence of magnetite and glycerol on charge storage. Results showed an increase of dielectric constant with the addition of these components.

Acknowledgments

The authors thank: the National Council for Scientific and Technological Development (CNPq), Coordination for the Improvement of Higher Level Personnel (CAPES) and The Minas Gerais State Research Foundation (FAPEMIG) for financial support; Departments of Chemistry, Physics, and Forest Science at Federal University of Lavras for their outstanding infrastructure support; USDA, Bioproducts from Agricultural Feedstocks, Project Number: 2030-41000-058-00-D; Marali Vilela Dias for tensile tests; Mário Guerreiro for FTIR and thermal analysis.

Bibliography

Abdul Khalil, H. P. S., Saurabh, C. K., A.S., A., Nurul Fazita, M. R., Syakir, M. I., Davoudpour, Y., … Dungani, R. (2016). A review on chitosan-cellulose blends and nanocellulose reinforced chitosan biocomposites: Properties and their applications. Carbohydrate Polymers, 150, 216–226. http://doi.org/http://dx.doi.org/10.1016/j.carbpol.2016.05.028

Ali-zade, R. A. (2015). Influence of Magnetic Field on Dielectric Permittivity of Nanocomposites on the Base of Polymeric Matrix: Collagen, Polystyrole, and Magnetite Nanoparticles. IEEE Transactions on Magnetics, 51(7), 1–8. http://doi.org/10.1109/TMAG.2015.2395998

Arantes, A. C. C., Almeida, C. das G., Dauzacker, L. C. L., Bianchi, M. L., Wood, D. F., Williams, T. G., … Tonoli, G. H. D. (2017). Renewable hybrid nanocatalyst from magnetite and cellulose for treatment of textile effluents. Carbohydrate Polymers, 8617(17). http://doi.org/10.1016/j.carbpol.2017.01.007

ASTM. (2002). D 882: Standard Test Method for Tensile Properties of Thin Plastic Sheeting. ASTM, 14, 1–10.

ASTM. (2016). E96/ E96M: Standard Test Methods for Water Vapor Transmission of Materials. ASTM, 16, 1–14. http://doi.org/10.1520/E0096

Ayala, G., Agudelo, A. C., Paz, J., & Vargas, R. A. (2011). Study of dc conductivity, transport mechanism, and dielectric relaxation in cassava starch membranes plasticized with glycerol. Ionics, 17(7), 647–652. http://doi.org/10.1007/s11581-011-0557-z

Bhatt, A. S., Krishna Bhat, D., & Santosh, M. S. (2010). Electrical and magnetic properties of chitosan-magnetite nanocomposites. Physica B: Condensed Matter, 405(8), 2078–2082. http://doi.org/10.1016/j.physb.2010.01.106

Boukheir, S., Len, A., Füzi, J., Kenderesi, V., Achour, M. E., Éber, N., … Outzourhit, A. (2017). Structural characterization and electrical properties of carbon nanotubes/epoxy polymer composites. Journal of Applied Polymer Science, 134(8), 1–8. http://doi.org/10.1002/app.44514

Bufalino, L., de Sena Neto, A. R., Tonoli, G. H. D., de Souza Fonseca, A., Costa, T. G., Marconcini, J. M., … Mendes, L. M. (2015). How the chemical nature of Brazilian hardwoods affects nanofibrillation of cellulose fibers and film optical quality. Cellulose, 22, 3657–3672. http://doi.org/10.1007/s10570-015-0771-3

Castelló, M. L., Dweck, J., & Aranda, D. A. G. (2009). Thermal stability and water content determination of glycerol by thermogravimetry. Journal of Thermal Analysis and Calorimetry, 97(2), 627–630. http://doi.org/10.1007/s10973-009-0070-z

Celebi, H., & Kurt, A. (2015). Effects of processing on the properties of chitosan/cellulose nanocrystal films. Carbohydrate Polymers, 133, 284–293. http://doi.org/10.1016/j.carbpol.2015.07.007

Cornell, R. M., & Schwertmann, U. (2003). The Iron Oxides (2nd ed.). Verlag: Wiley- VCH. http://doi.org/10.1002/3527602097.ch1

Costa, V. L. D., Costa, A. P., Amaral, M. E., Oliveira, C., Gama, M., Dourado, F., & Simões, R. M. (2016). Effect of hot calendering on physical properties and water vapor transfer resistance of bacterial cellulose films. Journal of Materials Science, 51(21), 9562–9572. http://doi.org/10.1007/s10853-016-0112-4

da Silva, A. L., da Silva, L. R. R., Camargo, I. de A., Agostini, D. L. da S., Denardin, J. C., Rosa, D. dos S., … Mazzetto, S. E. (2017). Superparamagnetic nano-biocomposites for application as dielectric resonator antennas. Materials Chemistry and Physics, 185, 104–113. http://doi.org/10.1016/j.matchemphys.2016.10.011

Dias, M. V., Machado Azevedo, V., Borges, S. V., Soares, N. D. F. F., De Barros Fernandes, R. V., Marques, J. J., & Medeiros, É. A. A. (2014). Development of chitosan/montmorillonite nanocomposites with encapsulated α-tocopherol. Food Chemistry, 165, 323–329. http://doi.org/10.1016/j.foodchem.2014.05.120

Han, S., Sun, Q., Zheng, H., Li, J., & Jin, C. (2016). Green and facile fabrication of carbon aerogels from cellulose-based waste newspaper for solving organic pollution. Carbohydrate Polymers, 136, 95–100. http://doi.org/10.1016/j.carbpol.2015.09.024

Hassan, E. A., Hassan, M. L., Abou-zeid, R. E., & El-Wakil, N. A. (2016). Novel nanofibrillated cellulose/chitosan nanoparticles nanocomposites films and their use for paper coating. Industrial Crops and Products, 93, 219–226. http://doi.org/10.1016/j.indcrop.2015.12.006

Hong, P.-Z., Li, S.-D., Ou, C.-Y., Li, C.-P., Yang, L., & Zhang, C.-H. (2007). Thermogravimetric analysis of chitosan. Journal of Applied Polymer Science, 105(2), 547–551. http://doi.org/10.1002/app.25920

Kongjao, S., Damronglerd, S., & Hunsom, M. (2010). Purification of crude glycerol derived from waste used-oil methyl ester plant. Korean Journal of Chemical Engineering, 27(3), 944–949. http://doi.org/10.1007/s11814-010-0148-0

Kötz, R., & Carlen, M. (2000). Principles and applications of electrochemical capacitors. Electrochimica Acta, 45(15), 2483–2498. http://doi.org/10.1016/S0013-4686(00)00354-6

Kumar, A., & Holuszko, M. (2016). Electronic Waste and Existing Processing Routes: A Canadian Perspective. Resources, 5(4), 35. http://doi.org/10.3390/resources5040035

Lamim, R., de Freitas, R. A., Rudek, E. I., Wilhelm, H. M., Cavalcanti, O. A., & Bresolin, T. M. B. (2006). Films of chitosan andN-carboxymethylchitosan. Part II: effect of plasticizers on their physiochemical properties. Polymer International, 55(8), 970–977. http://doi.org/10.1002/pi.1959

Leal, G. F., Ramos, L. A., Barrett, D. H., Curvelo, A. A. S., & Rodella, C. B. (2015). A thermogravimetric analysis (TGA) method to determine the catalytic conversion of cellulose from carbon-supported hydrogenolysis process. Thermochimica Acta, 616, 9–13. http://doi.org/10.1016/j.tca.2015.07.017

Li, N., Li, X., Yang, C., Wang, F., Li, J., Wang, H., … Li, D. (2016). Fabrication of a flexible free-standing film electrode composed of polypyrrole coated cellulose nanofibers/multi-walled carbon nanotubes composite for supercapacitors. RSC Advances, 6(89), 86744–86751. http://doi.org/10.1039/C6RA19529F

Liu, S., Yu, T., Wu, Y., Li, W., & Li, B. (2014). Evolution of cellulose into flexible conductive green electronics: a smart strategy to fabricate sustainable electrodes for supercapacitors. RSC Advances, 4(64), 34134. http://doi.org/10.1039/C4RA07017H

Liu, Y., Sun, B., Wang, Z., & Ni, Y. (2016). Mechanical and water vapor barrier properties of bagasse hemicellulose-based films. BioResources, 11(2), 4226–4236. http://doi.org/10.15376/biores.11.2.4226-4236

Luz, a. P., Ribeiro, S., & Pandolfelli, V. C. (2008). Use of the wettability in the investigation of the corrosion behaviour of the refractory materials. Cerâmica, 54(330), 174–183. http://doi.org/10.1590/S0366-69132008000200007

Morgado, J., Pereira, A. T., Bragança, A. M., Ferreira, Q., Fernandes, S. C. M., Freire, C. S. R., … Alcácer, L. (2013). Self-standing chitosan films as dielectrics in organic thin-film transistors. Express Polymer Letters, 7(12), 960–965. http://doi.org/10.3144/expresspolymlett.2013.94

Nishino, A. (1996). Capacitors: operating principles, current market and technical trends. Journal of Power Sources, 60(2), 137–147. http://doi.org/10.1016/S0378-7753(96)80003-6

Nowakowski, P. (2016). A proposal to improve e-waste collection efficiency in urban mining: Container loading and vehicle routing problems – A case study of Poland. Waste Management. http://doi.org/http://dx.doi.org/10.1016/j.wasman.2016.10.016

Owens, D. K., & Wendt, R. C. (1969). Estimation of the surface free energy of polymers. Journal of Applied Polymer Science, 13(8), 1741–1747. http://doi.org/10.1002/app.1969.070130815

Pang, S. C., Khoh, W. H., & Chin, S. F. (2011). Synthesis and Characterization of Magnetite/Carbon Nanocomposite Thin Films for Electrochemical Applications. Journal of Materials Science & Technology, 27(10), 873–878. http://doi.org/10.1016/S1005-0302(11)60158-8

Rana, G., Johri, U. C., & Asokan, K. (2013). Correlation between structural and dielectric properties of Ni-substituted magnetite nanoparticles. EPL (Europhysics Letters), 103, 17008. http://doi.org/10.1209/0295-5075/103/17008

Sanyang, M. L., Sapuan, S. M., Jawaid, M., Ishak, M. R., & Sahari, J. (2015). Effect of Plasticizer Type and Concentration on Dynamic Mechanical Properties of Sugar Palm Starch Based Films. International Journal of Polymer Analysis and Characterization, 5341(July), 150622104055002. http://doi.org/10.1080/1023666X.2015.1054107

Schwertmann, U., & Cornell, R. M. (2000). Iron Oxides in the Laboratory (Second). Verlag: Wiley- VCH.

Seoane, I. T., Fortunati, E., Puglia, D., Cyras, V. P., & Manfredi, L. B. (2016). Development and characterization of bionanocomposites based on poly(3-hydroxybutyrate) and cellulose nanocrystals for packaging applications. Polymer International, 65(9), 1046–1053. http://doi.org/10.1002/pi.5150

Shahbazi, M., Rajabzadeh, G., Rafe, A., Ettelaie, R., & Ahmadi, S. J. (2016). The physico-mechanical and structural characteristics of blend film of poly (vinyl alcohol) with biodegradable polymers as affected by disorder-to-order conformational transition. Food Hydrocolloids, 60, 393–404. http://doi.org/10.1016/j.foodhyd.2016.03.038

Share, K., Westover, A., Li, M., & Pint, C. L. (2016). Surface engineering of nanomaterials for improved energy storage – A review. Chemical Engineering Science, 154, 3–19. http://doi.org/10.1016/j.ces.2016.05.034

Silverstein, R. M., & Webster, F. X. (1997). Spectrometric Identification Organic Compounds (6th ed.). London: Jonh Wiley & Sons.

Su, C. (2017). Environmental implications and applications of engineered nanoscale magnetite and its hybrid nanocomposites: A review of recent literature. Journal of Hazardous Materials, 322, 48–84. http://doi.org/10.1016/j.jhazmat.2016.06.060

Tansel, B. (2017). From electronic consumer products to e-wastes: Global outlook, waste quantities, recycling challenges. Environment International, 98, 35–45. http://doi.org/10.1016/j.envint.2016.10.002

Thakur, V. K., & Voicu, S. I. (2016). Recent advances in cellulose and chitosan based membranes for water purification: A concise review. Carbohydrate Polymers, 146, 148–165. http://doi.org/10.1016/j.carbpol.2016.03.030

Tonoli, G. H. D., Holtman, K. M., Glenn, G., Fonseca, A. S., Wood, D., Williams, T., … Orts, W. J. (2016). Properties of cellulose micro/nanofibers obtained from eucalyptus pulp fiber treated with anaerobic digestate and high shear mixing. Cellulose, 23, 1239–1256. http://doi.org/10.1007/s10570-016-0890-5

Tonoli, G. H. D., Rodrigues Filho, U. P., Savastano, H., Bras, J., Belgacem, M. N., & Rocco Lahr, F. A. (2009). Cellulose modified fibres in cement based composites. Composites Part A: Applied Science and Manufacturing, 40(12), 2046–2053. http://doi.org/10.1016/j.compositesa.2009.09.016

Vellakkat, M., & Hundekal, D. (2017). Electrical conductivity and supercapacitor properties of polyaniline/chitosan/nickel oxide honeycomb nanocomposite. Journal of Applied Polymer Science, 134(9), 1–12. http://doi.org/10.1002/app.44536

Yoshida, C. M. P., Oliveira, E. N., & Franco, T. T. (2009). Chitosan tailor-made films: The effects of additives on barrier and mechanical properties. Packaging Technology and Science, 22(3), 161–170. http://doi.org/10.1002/pts.839

Yuan, Y., & Lee, T. R. (2013). Surface science techniques. (G. Bracco & B. Holst, Eds.)Springer Series in Surface Sciences (Vol. 51). Berlin: Springer Berlin Heidelberg. http://doi.org/10.1007/978-3-642-34243-1

Zeng, X., Yang, C., Chiang, J. F., & Li, J. (2017). Innovating e-waste management: From macroscopic to microscopic scales. Science of the Total Environment, 575, 1–5. http://doi.org/10.1016/j.scitotenv.2016.09.078

Zhu, X., Bao, L., Wei, Y., Ma, J., & Kong, Y. (2016). Removal of toxic indigo blue with integrated biomaterials of sodium carboxymethyl cellulose and chitosan. International Journal of Biological Macromolecules, 91, 409–415. http://doi.org/10.1016/j.ijbiomac.2016.05.097

CONSIDERAÇÕES FINAIS

Nesse trabalho foi estudado o desenvolvimento de híbridos nanoestruturados com foco em aplicações ambientais. A revisão de literatura apresentou diferentes possibilidades de aplicação dos materiais híbridos, definição dos componentes e formas de preparo. Depois foram apresentadas as características físicas e químicas de precursores da produção de híbridos, que foram a celulose, a magnetita e a quitosana, bem como a ocorrência, obtenção e forma de produção dos mesmos. Algumas aplicações ambientais para os híbridos foram apresentadas nas áreas de catálise e eletrônica.

Na área de catálise foi realizado um trabalho prático onde foi produzido um catalisador híbrido renovável de nanofibrilas de celulose e magnetita que tem potencial para ser usado em reações do tipo Fenton para degradação de poluentes orgânicos. Os íons ferro presentes na magnetita catalisaram a reação de geração de radicais hidroxila que degradaram o corante azul de metileno presente em efluentes têxteis.

Na área de eletrônica foi realizado um outro trabalho prático onde foram produzidos filmes finos contento nanofibrilas de celulose, quitosana, magnetita e glicerol. Os filmes produzidos apresentaram boas propriedades mecânicas e estabilidade térmica. Os filmes são renováveis e apresentam potencial para serem aplicados como dielétricos em capacitores.

Finalizando, a área de produção de materiais híbridos possui inúmeras possibilidades. Biopolímeros são bons precursores na produção de híbridos e esses componentes em escala nanométrica conferem características diferenciadas aos materiais. A magnetita também é uma boa precursora pois é um óxido de ferro versátil e de fácil obtenção.